frontiers | Frontiers in Marine Science

TYPE Original Research
PUBLISHED 08 December 2023
DOI 10.3389/fmars.2023.1270343

OPEN ACCESS

EDITED BY
Fabienne Marret,
University of Liverpool, United Kingdom

REVIEWED BY
Peter Bijl,
Utrecht University, Netherlands
Arief Rachman,
National Research and Innovation Agency, Indonesia

*CORRESPONDENCE
Ana Amorim
aaferreira@ciencias.ulisboa.pt
Iria García-Moreiras
iriagamo@uvigo.es

RECEIVED 31 July 2023
ACCEPTED 17 November 2023
PUBLISHED 08 December 2023

CITATION
García-Moreiras I, Hatherly M, Zonneveld K, Dubert J, Nolasco R, Santos AI, Oliveira A, Moita T, Oliveira PB, Magalhães JM and Amorim A (2023) New physical and biological evidence of lateral transport affecting dinoflagellate cyst distribution in the benthic nepheloid layer along a land-sea transect off Figueira da Foz (Atlantic Iberian margin). *Front. Mar. Sci.* 10:1270343. doi: 10.3389/fmars.2023.1270343

New physical and biological evidence of lateral transport affecting dinoflagellate cyst distribution in the benthic nepheloid layer along a land-sea transect off Figueira da Foz (Atlantic Iberian margin)

Iria García-Moreiras[1]*, Melissa Hatherly[2,3], Karin Zonneveld[4,5], Jesus Dubert[6,7], Rita Nolasco[6,7], Ana Isabel Santos[8], Anabela Oliveira[8,9], Teresa Moita[10], Paulo B. Oliveira[11], Jorge M. Magalhães[12,13] and Ana Amorim[2,3]*

[1]CIM – Centro de Investigación Mariña e Departamento de Bioloxía Vexetal e Ciencias do Solo, Facultade de Ciencias, Universidade de Vigo, Vigo, Spain, [2]MARE – Marine and Environmental Sciences Centre/ARNET – Aquatic Research Network, Faculdade de Ciências, Universidade de Lisboa, Lisbon, Portugal, [3]Departamento de Biologia Vegetal, Faculdade de Ciências, Universidade de Lisboa, Lisbon, Portugal, [4]Center for Marine Environmental Sciences (MARUM), University of Bremen, Bremen, Germany, [5]Geosciences Department, University of Bremen, Bremen, Germany, [6]Centre of Environmental and Marine Studies (CESAM), Departamento de Física e Centro de Estudos Do Ambiente e Do Mar, Universidade de Aveiro, Aveiro, Portugal, [7]IIM – Instituto de Investigacións Mariñas, Consejo Superior de Investigaciones Científicas (CSIC), Vigo, Spain, [8]IH – Instituto Hidrográfico, Marine Geology Division, Lisbon, Portugal, [9]Instituto Dom Luiz, Faculdade de Ciências, Universidade de Lisboa, Lisbon, Portugal, [10]CCMAR – Centro de Ciências do Mar, Universidade do Algarve, Faro, Portugal, [11]IPMA – Instituto Português do Mar e da Atmosfera, Algés, Portugal, [12]CIIMAR – Interdisciplinary Centre of Marine and Environmental Research, Universidade do Porto, Porto, Portugal, [13]Department of Geoscience, Environment and Spatial Planning (DGAOT), Faculty of Sciences, University of Porto, Porto, Portugal

Introduction: The production of resting cysts is a key dispersal and survival strategy of many dinoflagellate species. However, little is known about the role of suspended cysts in the benthic nepheloid layer (BNL) in the initiation and decline of planktonic populations.

Methods: In September 2019, sampling of the dinoflagellate cyst community at different water depths in the water column and in the bottom sediments, and studies of spatio-temporal changes in physical properties (temperature, salinity, density and suspended sediment concentration), were carried out along a land-sea transect off Figueira da Foz (NW Portugal) to investigate the dinoflagellate cyst distribution and the factors (physical and biological) affecting it. A clustering analysis was used to compare the BNL and sediment cyst records with the cyst rain recorded by a sediment trap at a fixed station. Furthermore, Lagrangian particle experiments enabled simulating cyst trajectories in the BNL 5 and 10 days before sampling and assessing cross-shore, vertical and alongshore transport within the studied region.

Results: A well-developed BNL was present during the survey, which covered a change from active (14th of September) to relaxed (19th of September) upwelling conditions. Organic-walled dinoflagellate cysts were dominant in all samples, although calcareous dinoflagellate cysts consistently occurred (at low abundances). High proportions of full cysts were observed in the BNL, of which a significant portion was viable as shown by excystment experiments. Moreover, BNL cyst records collected on the 19th of September along the land-sea transect were similar to the sediment trap cyst record but greatly differed from sediment cyst records. The heterotrophic small spiny brown cysts (SBC) and cysts of the autotrophic yessotoxin-producer *Protoceratium reticulatum* notably increased during the survey, in the BNL and in the water column above.

Discussion: The comparison of the BNL, surface sediment and sediment trap cyst records supported that the main origin of cysts in the BNL was the recent production in the water column. The spatial coincidences in the distribution of cysts and vegetative cells of *Protoceratium reticulatum* also supported that full cysts in the water column were being produced in surface waters. New data evidenced the presence of a significant reservoir of viable cysts in the BNL that have the potential to seed new planktonic blooms. Furthermore, back-track particle modelling evidenced that alongshore advection was the main physical mechanism controlling cyst dynamics in the BNL during most part of the survey period, being particularly intense in coastal stations (<100 m depth). Consequently, the sediment cyst signal is a mixture of locally and regionally produced cysts. We provide multi-disciplinary data evidencing that cysts recently formed in the photic zone can be laterally advected within the studied region through the BNL, contributing to a better understanding of the role of the BNL in cyst dynamics and tracing the seed sources of the new blooms.

KEYWORDS

benthic nepheloid layer, dinoflagellate cysts, cyst reservoir, advection, coastal ecosystems, Portuguese margin

1 Introduction

At least 13-16% of living dinoflagellate species can form long-term resistant structures (resting cysts) as part of their life cycle (Head, 1996). The alternation of a vegetative stage (motile cell) and a dormant phase (non-motile cyst) is a successful ecological strategy in highly changing environments such as coastal ecosystems, as cysts facilitate the species dispersal and survival during adverse conditions (e.g., Anderson, 1984; Dale, 1996; Smayda and Reynolds, 2003). In culture nutrient depletion can trigger cyst production of some dinoflagellate species (e.g., Blanco, 1995a; Figueroa and Bravo, 2005); however, in the field the highest cyst production occurs during and after bloom events, not necessarily accompanied by a decrease in nutrient inputs (Amorim et al., 2001; Peña-Manjarrez et al., 2009; Diaz et al., 2014; Brosnahan et al., 2017; Mertens et al., 2023). Cysts accumulated on the seabed can remain viable for a long time (Dale, 1983; Lundholm et al., 2011), after which they can be resuspended and provide the necessary inoculum for seeding planktonic populations (e.g., Nehring, 1996; Kremp, 2001; Anderson et al., 2005; Giannakourou et al., 2005; Anderson et al., 2014; Bravo and Figueroa, 2014; Mertens et al., 2023). Dinoflagellate cysts are non-motile and, after being produced in the upper water layers, act as passive particles that will eventually sink to the ocean floor (Dale, 1983; Joyce and Pitcher, 2004; Mertens et al., 2023). The sinking rate of the cysts under culture conditions was estimated to be ~6-11 m/day, although this could vary between different species due to their different morphology (Anderson et al., 1985). Pilskaln et al. (2014a) obtained a model-based estimate of the settling rate for individual *Alexandrium* cysts of 10 m/day in the Gulf of Maine. Unfortunately, *in-situ* observations of sinking speeds of dinoflagellate cysts are rare. Sediment trap studies performed in open ocean environments off Cape Blanc showed much higher cyst sinking rates (>274 m/day), agreeing with phytoplankton aggregate sinking speeds (Susek et al., 2005; Zonneveld et al., 2010). Several studies reported that a large part of the phytoplankton would be transported through the water column in the form of aggregates and fecal pellets that would significantly increase their sinking speeds (Smayda, 1971; Waite et al., 2000; Turner, 2002; Karakaş et al., 2009; Zonneveld et al., 2010). Furthermore, vertical (source-to-sink) trajectories of organic particles can be affected by lateral transport

(Freudenthal et al., 2001; Oliveira et al., 2007); this effect could be particularly relevant when considering ocean basin scale (Zonneveld et al., 2018; Nooteboom et al., 2019; Zonneveld et al., 2022) but of less impact in coastal areas and at the regional scale (Pilskaln et al., 2014a; Nooteboom et al., 2019).

Harmful algal blooms (HAB) are a recurrent feature on the Atlantic Iberian margin and may represent threats to human health, ecosystem quality and local economy (e.g., Tilstone et al., 1994; Moita and da Silva, 2001; Amorim et al., 2004; Álvarez-Salgado et al., 2008; Trainer et al., 2010; Ribeiro et al., 2012). Some of the HAB-forming dinoflagellate species and other potentially toxic species in this region are cyst producers, such as *Alexandrium minutum, Gymnodinium catenatum*, *Lingulodinium polyedra* and *Protoceratium reticulatum* (Anderson et al., 1988; Figueiras and Pazos, 1991; Blanco, 1995a; Blanco, 1995b; Moita and Vilarinho, 1999; Moita et al., 2003; Amorim et al., 2004; Bravo et al., 2010; Moita et al., 2022). The biological and physical mechanisms involved in the seeding and initiation of blooms (such as inoculum from cysts), may vary between species and are still not fully understood, although their assessment is critical for adequate monitoring and prediction of HABs, and coastal management (e.g., Bravo et al., 2010; Anderson, 2014; Berdalet et al., 2017; Brosnahan et al., 2020). The study region off Figueira da Foz is an area affected by recurrent blooms of *G. catenatum* (e.g., Botelho et al., 2019) however a cyst survey carried out in the area could not detect the presence of significant sediment cyst banks (García-Moreiras et al., 2021), suggesting local blooms may rely on other seeding strategies.

Nepheloid layers (NL) are zones of increased particle concentration (turbidity) and can significantly affect the transport of suspended particulate matter in the ocean (e.g., Oliveira et al., 2002; Zonneveld et al., 2018; Villacieros-Robineau et al., 2019). Benthic nepheloid layers (BNL) are assumed to be formed mainly from seabed particle resuspension, mostly induced by physical processes, such as upwelling/downwelling-induced currents and internal waves (Oliveira et al., 2002; Oliveira et al., 2007; Tian et al., 2022; Oliveira et al., 2023 and references therein). However, the origin and fate of the organic particles that form the NL and their role in the biota distribution are still poorly understood. Studies have shown that the BNL can be enriched in suspended viable cysts, which may serve as inoculum to seed planktonic blooms (Nehring, 1996; Pilskaln et al., 2014b).

The present work was motivated by the little knowledge available on particle transport in coastal environments of the Atlantic Iberian margin and the need for new data that help understand the role of suspended cysts in the BNL in the initiation and decline of dinoflagellate blooms. In September 2019, sampling of the dinoflagellate cyst community at different water depths in the water column and in the bottom sediments, and studies of spatio-temporal changes in physical properties (temperature, salinity, density and suspended sediment concentration), were carried out along a land-sea transect off Figueira da Foz (NW Portugal). The main objectives were: 1) to investigate BNL development and characterize dinoflagellate cyst abundance and diversity; 2) to detect the presence of viable cysts in the BNL, and 3) to study the main physical and biological processes affecting cyst distribution in the BNL.

Cyst records were compared with the cyst rain recorded by a sediment trap and cyst distribution in the underlying sediments by statistical methods, to investigate the origin of cysts in the BNL. Moreover, excystment experiments were carried out to check the viability of full cysts. Particle back-track Lagrangian experiments enabled reconstructing the trajectory of cysts in the BNL, providing new insights into their origin and the transport processes affecting their distribution in coastal environments.

2 Study site

2.1 General environmental settings

The land-sea transect is located off Figueira da Foz on the Portuguese coast (Atlantic Iberian margin), between the longitudes 8.85°W and 9.50°W, and at a latitude of ~40.20° N (Figure 1A). In Northern Portugal, the climate is Mediterranean with dry warm summers and wet cool winters (Mora and Vieira, 2020). Together with fluvial contributions, upwelling is the most relevant factor controlling regional hydrodynamics and phytoplankton dynamics (e.g., Moita, 1993; Moita et al., 2003; Oliveira et al., 2019; Ferreira et al., 2021; Santos et al., 2021). The upwelling intensification and relaxation cycles modulate the sea-surface temperature (SST) distribution, the water column stratification and the nutrient availability in the euphotic zone and therefore phytoplankton growth (Fraga et al., 1988; Oliveira et al., 2009a). Furthermore, local hydrography and phytoplankton distribution are strongly affected by mesoscale processes, such as eddies, upwelling filaments, fronts and internal waves (Relvas et al., 2007; Rossi et al., 2013; Oliveira et al., 2019).

Upwelling is more frequent and intense from late spring to early autumn when northerly winds prevail (Fiúza et al., 1982; Peliz et al., 2002). The intensification of equatorward winds drives an alongshore current (Equatorward jet) that dominates the coastal circulation, and an inshore transport through the bottom nepheloid layer (BNL) associated with the Ekman dynamics. Under the upwelling influence, coastal environments are characterized by marked land-sea environmental gradients, with colder waters inshore and SST increasing seawards (e.g., Oliveira et al., 2009a; Oliveira et al., 2019).

More offshore on the outer shelf and the slope, a saltier and warmer current flows in the opposite direction to the Equatorward jet, the Iberian Poleward Current or IPC (Peliz et al., 2005; Otero et al., 2008; Teles-MaChado et al., 2015). During upwelling events, the IPC can be debilitated and translocated offshore, as the low-salinity and colder water mass formed by river discharge and continental run-off —the Western Iberian Buoyant Plume (WIBP)— is stretched offshore. In contrast, the warmer IPC is intensified with upwelling (and equatorward winds) relaxation, when offshore warmer waters migrate inshore (e.g., Peliz et al., 2005; Ferreira Cordeiro et al., 2018).

The closest contribution of freshwater and fluvial sediments to the study area is the Mondego River, with a catchment basin of 6670 km^2 and an estimated annual average runoff up to ~150 m^3s^{-1} (Cunha and Dinis, 2002). However, the Douro and Minho Rivers

10.3389/fmars.2023.1270343

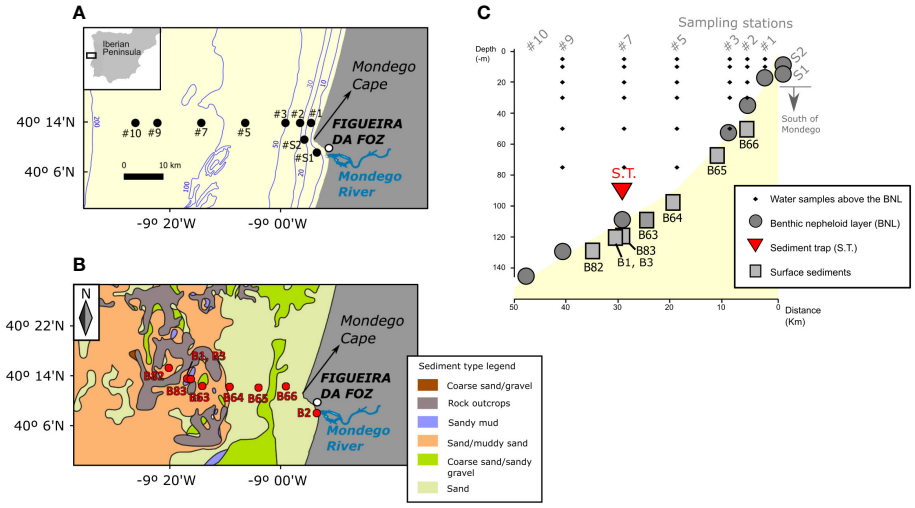

FIGURE 1
Study site off Figueira da Foz (Atlantic Iberian margin) and cyst sampling locations. Water sampling stations **(A)** are superimposed on the bathymetric contours (in meters) taken from the General Bathymetric Chart of the Oceans (https://www.gebco.net/). Sediment sampling stations **(B)** are superimposed on the Seabed Substrate map from Emodnet Geology (https://drive.emodnet-geology.eu/geoserver/gtk/wfs). **(C)** Vertical view of the sampled points in the benthic nepheloid layer (BNL), the water column above the BNL, the sediment trap (S.T.) and the underlying surface sediments. **(A, B)** were redrawn from García-Moreiras et al. (2021), © 2021 García-Moreiras I, Oliveira A, Santos AI, Oliveira PB and Amorim A, published in Frontiers in Marine Science under a CC by 4.0 license (hyperlink: https://creativecommons.org/licenses/by/4.0/#).

further north of the study site are the greater contributors to the WIBP on the NW Iberian coast (Mendes et al., 2016).

High-amplitude internal waves promote an increase in turbulence in the water column and may disturb the ocean bottom resulting in higher turbidity and changes in BNL thickness (Oliveira et al., 2007; Quaresma et al., 2007; Oliveira et al., 2023). The study area was selected because of its location in a naturally occurring interaction hotspot of Internal Solitary Waves (ISW) (Magalhaes et al., 2021). ISW dynamics may thus be relevant for the understanding of particle transport through the BNL in the studied area. ISW are mainly generated by tides and their interaction with bottom topography (e.g., Magalhaes et al., 2021). Their propagation, which can last for a few days in the studied region, occurs along the oceanic pycnocline and its characteristics can vary significantly due to mesoscale variability (Oliveira et al., 2019). Off Figueira da Foz, ISW variability (amplitude) is comparable to the semidiurnal tidal cycle (Magalhaes et al., 2021; Magalhaes et al., 2022).

Phytoplankton assemblages in the Iberian upwelling system typically change from diatom dominance during active upwelling (spring-summer) to dinoflagellate dominance as upwelling relaxes (late-summer to autumn transition). Dinoflagellates are usually favored after upwelling events, as stratification increases and surface waters are still warm and rich in nutrients (e.g., Fraga et al., 1988; Tilstone et al., 2000; Amorim et al., 2001; Figueiras et al., 2002; Amorim et al., 2004; Crespo et al., 2006; Bravo et al., 2010; Smayda and Trainer, 2010). On a spatial scale, abundances of dinoflagellates and other flagellates generally increase over diatoms in more stratified waters in the transition between coastal upwelling and offshore warmer waters (e.g., Oliveira et al., 2009b), and at the inshore side of the upwelling front (Tilstone et al., 1994; Moita et al., 2003).

2.2 Oceanography and phytoplankton distribution in the study site prior to the BNL sampling

Distributions of satellite-derived Chl-*a* concentration (Figure 2A) and SST (Figure 2B) from the Copernicus Marine Service (CMEMS) (https://data.marine.copernicus.eu/viewer/) reflected the progression of an upwelling event that peaked on the 11th-12th of September and relaxed in the following days. According to *in-situ*, satellite-derived and modelling data investigated by Nunes (2021), during this upwelling event, the mixed layer had a depth of 20-30 m and the predominant surface currents (<20 m depth) near the coast were equatorward. Current velocities were higher near the coast and decreased offshore. A water mass of higher primary productivity (maximal Chl-*a* concentrations of ~3-5 mg/m^3) was separated from the coast by a narrow band of colder waters with lower productivity (Nunes et al., 2022). A maximum divergence zone was detected near the coast (at ~5 km to the coastline) on the 10th of September, which moved further offshore over time as upwelling progressed (Nunes, 2021). The development of a series of complex upwelling filaments running offshore was also observed (Figures 2A, B).

Spatio-temporal variability of phytoplankton communities and nutrients was investigated along the same land-sea transect by Moita et al. (2022). On the 12th of September, two days before the cyst sampling, a bloom of *Protoceratium reticulatum* was well established at mid-shelf (around 20 m depth isobath), with maximum cell concentrations of 2.3×10^3 cells l^{-1}. The bloom was located in warmer and stratified (but not nutrient-depleted) waters separated from the coast by upwelled colder waters. Other HAB species were blooming at the same time, such as the non-cyst-forming dinoflagellate *Dinophysis acuta* (below *P. reticulatum*

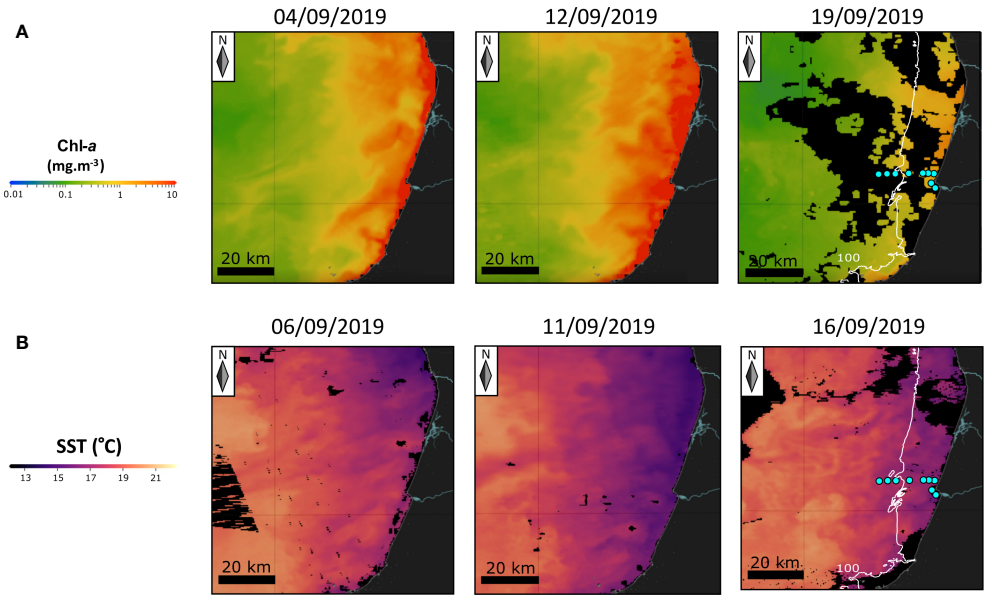

FIGURE 2
Surface distributions of chlorophyll-*a* concentration **(A)** and temperature **(B)** off Figueira da Foz before and during the BNL sampling campaign. Satellite-derived data were taken from the Copernicus Marine Service (CMEMS) website (https://data.marine.copernicus.eu/viewer/). Areas where clouds made data collection impossible are shown in black. On the right diagrams, sampled sites (blue dots) and the 100-m isobath (white line) are represented.

bloom) and species of the diatom genus *Pseudo-nitzschia* (in the inshore colder waters). Maximal values of phytoplankton biomass were always detected above the pycnocline. On the 19th of September, phytoplankton blooms migrated inshore as upwelling relaxed and surface warmer waters approached the coast (Moita et al., 2022).

3 Materials and methods

Between 14th and 19th September 2019, environmental data and water and sediment samples for dinoflagellate cyst analyses were collected onboard the NRP Auriga during the Hydrographic Institute (IH)-HABWAVE cruise. Sampling stations were located at different water depths following an inshore-offshore transect off Figueira da Foz, on the NW Portuguese coast (Atlantic Iberian margin) (Figures 1A–C). Furthermore, using a numerical modelling configuration, Lagrangian experiments enabled simulating cyst trajectories in the benthic nepheloid layer (BNL) 5 and 10 days before sampling and assessing cross-shore, vertical and alongshore transport within the studied region.

3.1 *In-situ* data acquisition

3.1.1 Oceanographic data

Temperature, conductivity, depth and turbidity, were profiled at the different sampling stations along the transect with an Idronaut 320 plus CTD associated with a Seapoint turbidity meter on the 14th and 19th of September, 2019. Turbidity (in NTU- Nepheloid Turbidity Units) was calibrated in suspended sediment concentration (SSC) with water samples collected at the bottom nepheloid layer (33 samples). The water samples were filtered on board using pre-weighted acetate filters (porosity 0.45 µm and 47 mm). The turbidity profiles were converted into SSC (mg/l) using the following equation: SSC=0.976 x NTU. Additionally, environmental time series were recorded in a fixed station at the 110 m isobath (station #7, Figures 1A, C) on the 16th and 18th of September. Station 7 was selected based on previous time series analysis of SAR (Synthetic Aperture Radars) images from Sentinel 1 (Magalhaes et al., 2021). Data was acquired with a CTD/nephelometer (yoyo) and water samples for determination of particulate matter concentration were collected with a rosette firing system with 11 Niskin bottles (8 of 5.0 l and 3 of 2.5 l), covering two semi-diurnal low tides (33 yoyos on 16th September and 15 yoyos on 18th September, corresponding to, approximately, a 9-hour and 6-hour periods, respectively) (Oliveira A. et al., 2020). Additionally at this site, a mooring was deployed from 7th to 19th September 2019 with five self-recording thermistors and two ADCPs. The up-looking 300 kHz and the 1200 kHz ADCPs were mounted in a dual frame at ~100 m depth (Oliveira P.B. et al., 2020). The mooring included a sediment trap (area=0.015 m^2) at 90 m depth to record the export production of dinoflagellate cysts from 7th to 19th September 2019 (S.T. in Figure 1C; Table 1).

3.1.2 Water samples for cyst and phytoplankton studies

Water samples from the BNL for cyst analyses were collected with a rosette firing system equipped with a CTD/nephelometre. In the BNL, a total of 14 water samples for cyst analyses were collected on 14th and 19th September 2019 (Table 1). Selection of sampling depths for cyst analyses in the BNL was based on the turbidity signal

10.3389/fmars.2023.1270343

TABLE 1 Sampling campaign (IH)-HABWAVE, September 2019.

		Sample label	Type of sample	Station	Depth (m)	Sampled depth (m)	Sampling date (day/month/year)	Sampling time
Sediment trap	Cyst rain	S.T.	Water (sediment trap)	#7	114.3	90	7/9/2019 (14:04) to 19/09/2019 (09:18)	
BNL (land-sea transects)	Transect 1 (14/09/2019)	S1	Water	#S1	13.3	10	14/09/2019	5:45
		S2	Water	#S2	15.9	15.1	14/09/2019	6:35
		T1-1	Water	#1	15.6	15	14/09/2019	7:45
		T1-2	Water	#2	37.4	35	14/09/2019	8:36
		T1-3	Water	#3	52.2	50	14/09/2019	9:38
		T1-7	Water	#7	114.3	110	14/09/2019	13:14
		T1-9	Water	#9	132.7	130	14/09/2019	14:54
		T1-10	Water	#10	145.6	145	14/09/2019	15:53
	Transect 2 (19/09/2019)	T2-1	Water	#1	15.6	15	19/09/2019	7:41
		T2-2	Water	#2	37.4	35	19/09/2019	8:31
		T2-3	Water	#3	52.2	50	19/09/2019	9:08
		T2-5	Water	#5	86.0	80	19/09/2019	10:45
		T2-7	Water	#7	114.3	110	19/09/2019	12:38
		T2-9	Water	#9	132.7	130	19/09/2019	14:35
BNL Fixed point (Station #7)	Time series on 16/09/2019	F1-2 UP	Water	#7	114.3	83	16/09/2019	12:14
		F1-2 LOW	Water	#7	114.3	110	16/09/2019	12:14
		F1-3	Water	#7	114.3	108	16/09/2019	14:31
		F1-4 UP	Water	#7	114.3	95	16/09/2019	16:57
		F1-4 LOW	Water	#7	114.3	111	16/09/2019	16:57
	Time series on 16/09/2019	F2-0	Water	#7	114.3	110	18/09/2019	8:41
		F2-1	Water	#7	114.3	110	18/09/2019	9:03
		F2-2	Water	#7	114.3	110	18/09/2019	9:35
		F2-3	Water	#7	114.3	109	18/09/2019	9:56
		F2-4	Water	#7	114.3	100	18/09/2019	10:27
		F2-5	Water	#7	114.3	100	18/09/2019	10:50
		F2-6	Water	#7	114.3	105	18/09/2019	11:11
		F2-7	Water	#7	114.3	108	18/09/2019	11:30
		F2-8	Water	#7	114.3	100	18/09/2019	11:53
		F2-9	Water	#7	114.3	100	18/09/2019	12:13
		F2-10	Water	#7	114.3	95	18/09/2019	12:36
		F2-11	Water	#7	114.3	109	18/09/2019	12:56
		F2-12	Water	#7	114.3	109	18/09/2019	13:16
Planktonic samples above the BNL (land-sea transects)	Transect 1 (14/09/2019)	PS1.1	Water	#S1	13.3	5	14/09/2019	5:37
		PS1.2	Water	#S1	13.3	10	14/09/2019	5:37
		PS2.1	Water	#S2	15.9	5	14/09/2019	6:29

(Continued)

10.3389/fmars.2023.1270343

TABLE 1 Continued

		Sample label	Type of sample	Station	Depth (m)	Sampled depth (m)	Sampling date (day/month/year)	Sampling time
Sediment trap	Cyst rain	S.T.	Water (sediment trap)	#7	114.3	90	7/9/2019 (14:04) to 19/09/2019 (09:18)	
		PS2.3	Water	#S2	15.9	10	14/09/2019	6:29
		T1-P1.1	Water	#1	15.6	5	14/09/2019	7:41
		T1-P1.2	Water	#1	15.6	10	14/09/2019	7:41
		T1-P2.1	Water	#2	37.4	5	14/09/2019	8:35
		T1-P2.2	Water	#2	37.4	10	14/09/2019	8:35
		T1-P2.3	Water	#2	37.4	20	14/09/2019	8:35
		T1-P2.4	Water	#2	37.4	30	14/09/2019	8:35
		T1-P3.1	Water	#3	52.2	5	14/09/2019	9:36
		T1-P3.2	Water	#3	52.2	10	14/09/2019	9:36
		T1-P3.3	Water	#3	52.2	20	14/09/2019	9:36
		T1-P3.4	Water	#3	52.2	30	14/09/2019	9:36
		T1-P3.5	Water	#3	52.2	50	14/09/2019	9:36
		T1-P5.1	Water	#5	86.0	5	14/09/2019	11:29
		T1-P5.2	Water	#5	86.0	10	14/09/2019	11:29
		T1-P5.3	Water	#5	86.0	20	14/09/2019	11:29
		T1-P5.4	Water	#5	86.0	30	14/09/2019	11:29
		T1-P5.5	Water	#5	86.0	50	14/09/2019	11:29
		T1-P5.6	Water	#5	86.0	75	14/09/2019	11:29
		T1-P7.1	Water	#7	114.3	5	14/09/2019	13:12
		T1-P7.2	Water	#7	114.3	10	14/09/2019	13:12
		T1-P7.3	Water	#7	114.3	20	14/09/2019	13:12
		T1-P7.4	Water	#7	114.3	30	14/09/2019	13:12
		T1-P7.5	Water	#7	114.3	50	14/09/2019	13:12
		T1-P7.6	Water	#7	114.3	75	14/09/2019	13:12
		T1-P9.1	Water	#9	132.7	5	14/09/2019	14:51
		T1-P9.2	Water	#9	132.7	10	14/09/2019	14:51
		T1-P9.3	Water	#9	132.7	20	14/09/2019	14:51
		T1-P9.4	Water	#9	132.7	30	14/09/2019	14:51
		T1-P9.5	Water	#9	132.7	50	14/09/2019	14:51
		T1-P9.6	Water	#9	132.7	75	14/09/2019	14:51
	Transect 2 (19/09/2019)	P2-S1.1	Water	#S1	13.3	5	19/09/2019	6:01
		P2-S1.1	Water	#S1	13.3	10	19/09/2019	6:01
		P2-S2	Water	#S2	15.9	5	19/09/2019	6:33
		P2-S2.2	Water	#S2	15.9	10	19/09/2019	6:33
		P2-S2.3	Water	#S2	15.9	14	19/09/2019	6:33

(Continued)

10.3389/fmars.2023.1270343

TABLE 1 Continued

		Sample label	Type of sample	Station	Depth (m)	Sampled depth (m)	Sampling date (day/month/year)	Sampling time
Sediment trap	Cyst rain	S.T.	Water (sediment trap)	#7	114.3	90	7/9/2019 (14:04) to 19/09/2019 (09:18)	
		T2-P1.1	Water	#1	15.6	5	19/09/2019	7:37
		T2-P1.2	Water	#1	15.6	10	19/09/2019	7:37
		T2-P2.1	Water	#2	37.4	5	19/09/2019	8:27
		T2-P2.2	Water	#2	37.4	10	19/09/2019	8:27
		T2-P2.3	Water	#2	37.4	20	19/09/2019	8:27
		T2-P2.4	Water	#2	37.4	30	19/09/2019	8:27
		T2-P3.1	Water	#3	52.2	5	19/09/2019	9:25
		T2-P3.2	Water	#3	52.2	10	19/09/2019	9:25
		T2-P3.3	Water	#3	52.2	20	19/09/2019	9:25
		T2-P3.4	Water	#3	52.2	30	19/09/2019	9:25
		T2-P3.5	Water	#3	52.2	50	19/09/2019	9:25
		T2-P5.1	Water	#5	86.0	5	19/09/2019	11:00
		T2-P5.2	Water	#5	86.0	10	19/09/2019	11:00
		T2-P5.3	Water	#5	86.0	20	19/09/2019	11:00
		T2-P5.4	Water	#5	86.0	30	19/09/2019	11:00
		T2-P5.5	Water	#5	86.0	50	19/09/2019	11:00
		T2-P5.6	Water	#5	86.0	75	19/09/2019	11:00
		T2-P7.1	Water	#7	114.3	5	19/09/2019	12:57
		T2-P7.2	Water	#7	114.3	10	19/09/2019	12:57
		T2-P7.3	Water	#7	114.3	20	19/09/2019	12:57
		T2-P7.4	Water	#7	114.3	30	19/09/2019	12:57
		T2-P7.5	Water	#7	114.3	50	19/09/2019	12:57
		T2-P7.6	Water	#7	114.3	75	19/09/2019	12:57
		T2-P9.1	Water	#9	132.7	5	19/09/2019	14:52
		T2-P9.2	Water	#9	132.7	10	19/09/2019	14:52
		T2-P9.3	Water	#9	132.7	20	19/09/2019	14:52
		T2-P9.4	Water	#9	132.7	30	19/09/2019	14:52
		T2-P9.5	Water	#9	132.7	50	19/09/2019	14:52
		T2-P9.6	Water	#9	132.7	75	19/09/2019	14:52
Sediment samples (land-sea transect) (this study)		B1	Sediment	#7	114.3	114.3	16/09/2019	8:28
		B2	Sediment	#MH	11.0	11	18/09/2019	16:37
		B3	Sediment	#7	114.3	114.3	19/09/2019	16:55
IH/AQUIMAR (March 2019) Sediment samples (land-sea transect) (Garcia-Moreiras et al., 2021)		B63	Sediment	B63	102.2	102.2	21/3/2019	11:33
		B64	Sediment	B64	86.6	86.6	21/3/2019	11:04
		B65	Sediment	B65	62.1	62.1	23/3/2019	18:59

(Continued)

TABLE 1 Continued

		Sample label	Type of sample	Station	Depth (m)	Sampled depth (m)	Sampling date (day/month/year)	Sampling time
Sediment trap	Cyst rain	S.T.	Water (sediment trap)	#7	114.3	90	7/9/2019 (14:04) to 19/09/2019 (09:18)	
		B66	Sediment	B66	40.4	40.4	23/3/2019	18:31
		B82	Sediment	B82	117.8	117.8	21/3/2019	12:31
		B83	Sediment	B83	111.9	111.9	21/3/2019	11:53

Details of all samples collected in water and sediments for cyst analyses.

obtained during downcast (Figures 3, 4). At station #7, 19 additional samples were collected in the BNL at regular time intervals on 16th and 18th of September to record temporal variation (covering a period of ~5 hours each day). With the objective of better understanding the oceanographic processes underlying cyst dynamics in the BNL, these samples were collected in alternation with the complementary data acquisition yoyos referred above.

In some cases, the amplitude of the BNL indicated by the nephelometre during downcast allowed taking 2 samples, one at the lower and the other at the upper limits of the layer of increased particle density. In these cases, the prefix "up" or "low" was added to the sample label (Table 1). Water samples (40 – 47 L) were sieved on board through a 10 µm phytoplankton net (Hydrobios, Kiel, Germany) to concentrate the cysts. The concentrated samples were then stored in plastic bottles (70-159 ml) and kept in dark and cold (-4 °C) conditions until further processing (modified from Pilskaln et al., 2014b).

As referred above, at station #7, a mooring with a sediment trap was set to record the export production of dinoflagellate cysts from 7th to 19th September 2019 (S.T. in Figure 1C; Table 1).

At stations #1, #2, #3, #5, #7 and #9, additional water samples were collected for studying the vertical distribution of phytoplankton and cysts in the water column above the BNL (5, 10, 20, 30, 50 and 75 m, depending on station depth) (Figure 1C). These samples were preserved with hexamethylenetetramine buffered formalin until being analyzed in the laboratory (see Moita et al., 2022 for more details).

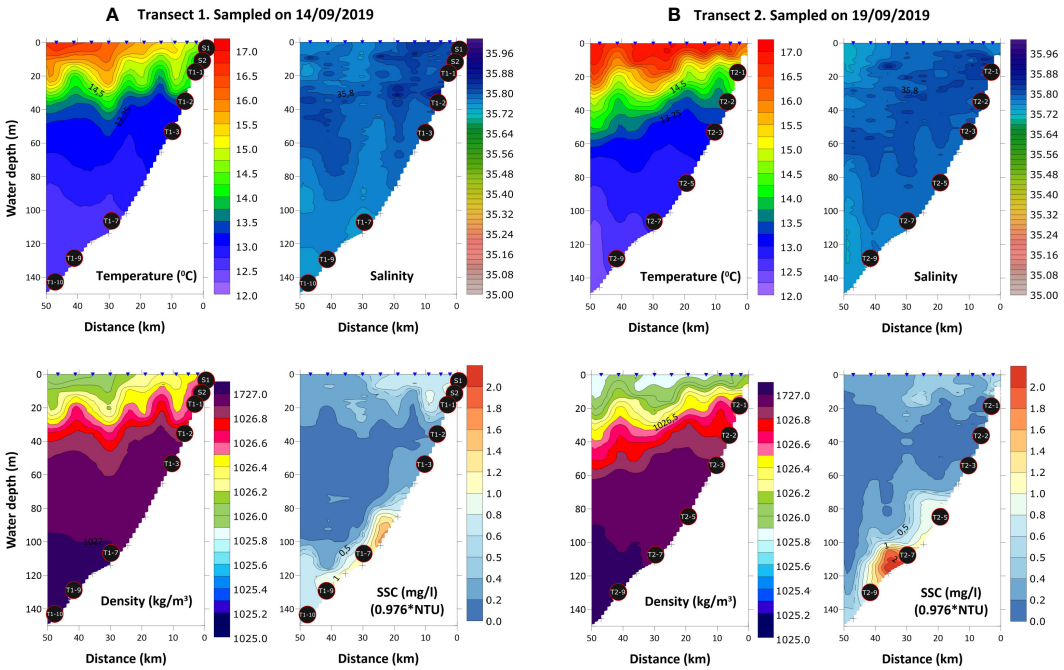

FIGURE 3
CTD profiles of temperature, salinity, density and suspended sediment concentration (SSC) along two transects, 14th **(A)** and 19th **(B)** September 2019, sampled off Figueira da Foz. Black circles indicate the position of the samples collected in the benthic nepheloid layer (BNL). Sample labels are according to Table 1.

10.3389/fmars.2023.1270343

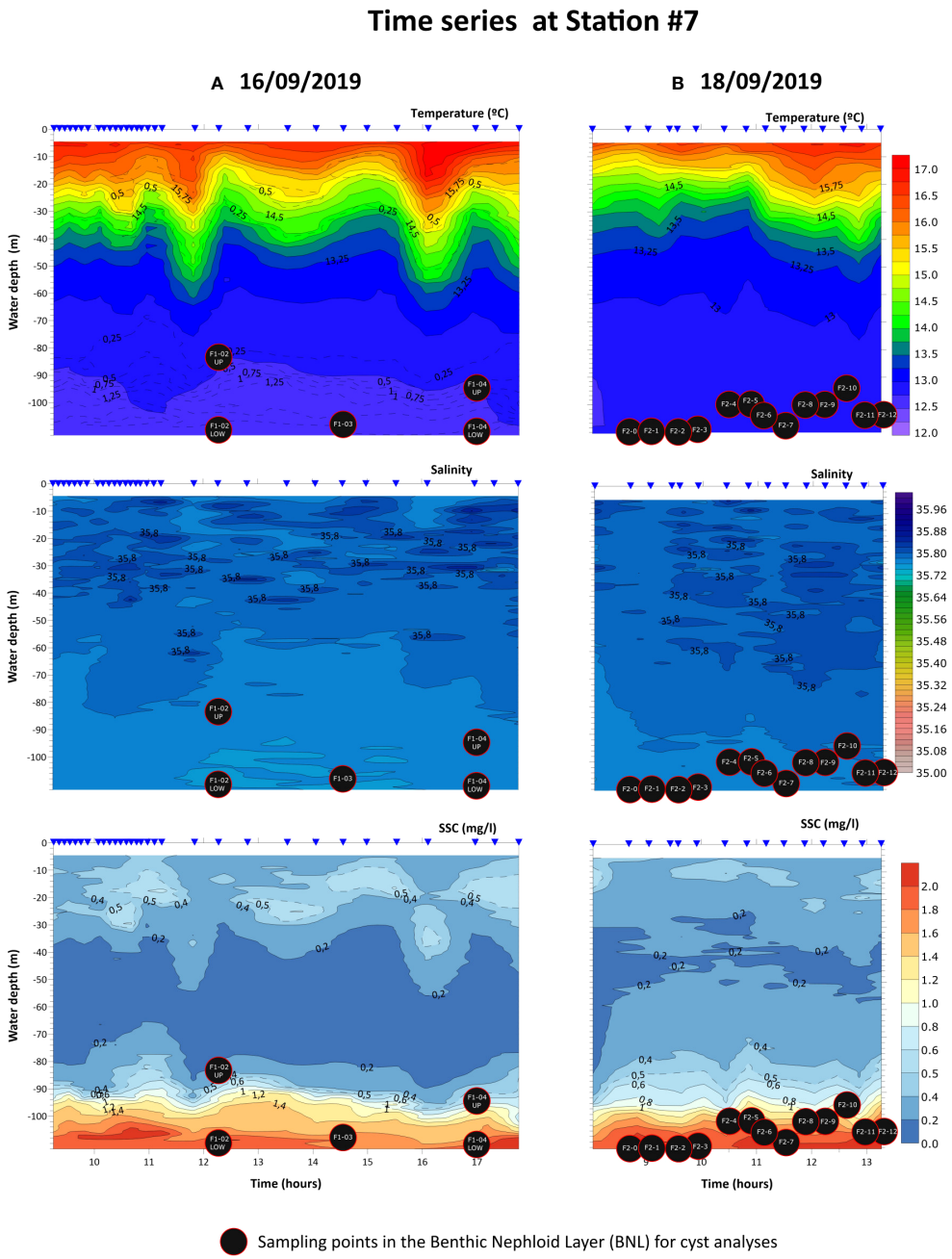

FIGURE 4
Fixed station CTD profiles of temperature, salinity, density and suspended sediment concentration (SSC) during part of the days 16th **(A)** and 18th **(B)** of September 2019 at station #7. Black circles indicate the sampled points in the BNL, labelled as in Table 1.

3.1.3 Sediment samples for cyst counts

Surface sediments for cyst analyses were sampled with a Smith McIntyre grab during two different campaigns. Plexiglass tubes (3.6 cm internal diameter) were inserted in the sediment and the top 1-cm layer was collected and stored at 4 °C in the dark for further analysis in the laboratory. Three sediment samples were obtained during the IH-HABWAVE campaign in September 2019: two at station #7 and one at the mouth of the Mondego River (B1, B2 and B3; Figure 1B). These sediment cyst records come from new analyses presented here for the first time. The other 6 sediment samples (B82, B83 and B63-66, Figures 1B, C) were collected in March 2019 during the IH/AQUIMAR cruise, and the cyst records are published in García-Moreiras et al. (2021).

All details of samples collected in water and sediments for cyst analyses (sample label, type of sample, sampling date and time, sampling station, sampled depth, etc.) were summarized in Table 1.

3.2 Sample processing and cyst analyses

3.2.1 Water samples

In the laboratory, water samples from the BNL were gently sonicated (60s) (Elmasonic S50R, Elma Schmidbauer GmbH) followed by centrifugation at 3600 rpm (~2510 g) (Eppendorf 5804 R), for 15 min (18°C) in graduated centrifuge tubes to concentrate the cysts (adapted from Kirn et al., 2005; Pilskaln et al., 2014a). The supernatant was removed to a known final volume adjusted between 1-40 ml with filtered seawater, depending on cyst concentration. In the case of the sediment trap sample, after homogenizing the whole sample (278 ml), a subsample of 10 ml was sonicated for 60s and sieved through a 150 µm-Nylon mesh onto a 20 µm-calibrated stainless steel mesh (Retsch). In both BNL and sediment trap samples, a volume of 1 or 2 ml was observed in an inverted light microscope (Leica DMi1) at x200 and x400 magnification.

Water samples collected above the BNL were subsampled (50ml) and analyzed by the Utermöhl technique (Hasle, 1978), under a Zeiss Vert.A1 equipped with phase contrast and bright field illumination, at 200x and 400x magnifications. Results for dinoflagellate cyst concentration are presented for each sampled depth and as the integrated water-column mean. In the second case, one composite sample per station was obtained by mixing a volume of the water samples from each depth in proportion to the height of the water column they represented (Venrick, 1978).

3.2.2 Sediment samples

A replicate of each sample (2 to 30 ml, depending on cyst concentration) was subsampled and processed as described in detail in García-Moreiras et al. (2021). In brief, sediment sample processing included gentle sonication (60 s), wet sieving (150 µm and 20 µm meshes) and density separation with sodium polytungstate (2.016 g/ml) (Bolch, 1997; Amorim et al., 2001). Samples were centrifuged and adjusted to a final volume of 1 to 10 ml with filtered sea water in Falcon tubes. Replicated sediment samples were used for the dry weight (drying at 60 °C until constant weight) and % moisture determination. The sample dry weight was determined using the previously calculated % moisture. As for BNL and trap samples, a volume of 1 or 2 ml was observed in an inverted Leica DMi1 microscope, at x200 and x400 magnifications.

In samples from BNL, sediment trap and surface sediments, dinoflagellate cysts were identified and counted in one or more 1-ml Sedgewick Rafter chambers (Graticules Optics, United Kingdom). Aliquots of all cyst samples were mounted on microscope slides with glycerine jelly and sealed with wax to take photographs and be stored as part of the permanent collection. Microphotographs (Plate 1) were obtained using an Olympus BX50 microscope and a Zeiss Axiocam HRc camera.

Total cyst sums (~100-800 cysts) included both empty and full (with cell contents) cysts. Results were expressed as relative abundances (percentage values of the total cyst assemblage) in both water and sediment samples. Moreover, absolute abundances (cyst concentrations in BNL and sediment samples, and cyst fluxes in the trap sample) were also calculated as follows:

- Cyst concentrations in BNL samples:

$$\frac{Cysts}{l} = \frac{\frac{counted\ \ cysts\ \ per\ \ sample}{counted\ \ volume\ \ (ml)} * final\ \ volume\ \ (ml)}{filtered\ \ volume\ \ (l)}$$

- Cyst concentrations in sediment samples:

$$\frac{Cysts}{g} = \frac{\frac{counted\ \ cysts\ \ per\ \ sample}{counted\ \ volume\ \ (ml)} * final\ \ volume\ \ (ml) * dilution\ \ factor}{dry\ \ weight\ \ of\ \ processed\ \ sample\ \ (g)}$$

- Cyst fluxes in the sediment trap sample:

$$\frac{Cysts}{\frac{m^2}{day}} = \frac{\frac{\frac{counted\ \ cysts\ \ per\ \ sample}{counted\ \ volume\ \ (ml)} * final\ \ volume\ \ (ml)}{sediment\ \ trap\ \ area\ \ (m^2)}}{time\ \ (days)}$$

3.3 Statistical analyses

To investigate the possible interaction between cysts in the 3 compartments —i.e., water column, BNL and surface sediments— a comparison of dinoflagellate cyst records was performed using clustering. Hierarchical cluster analysis was applied on square-root- transformed dinoflagellate cyst percentages using the Pvclust package (Suzuki et al., 2022) developed for R software v. 4.2.1. (R Development Core Team, 2013). The significance of the clusters obtained was tested by permutation tests (10000 permutations) that calculated the p-value via multiscale bootstrap resampling. Various classifications using different methods and distance matrices were developed, and finally the most significant clustering with the highest p-value was chosen.

A simple linear regression analysis was also used to compare cyst distribution in the BNL with the vegetative cell distribution of known cyst-producing dinoflagellates in the above water column, using the Microsoft Excel (2010) software. The regression coefficient (R^2) has been plotted as a measure of the significance of the regression analysis.

3.4 Dinoflagellate cyst taxa identification, nomenclature and excystment experiments

Dinoflagellate cyst identification and nomenclature followed: Zonneveld and Pospelova (2015); Gurdebeke et al. (2019); Mertens et al. (2020) and van Nieuwenhove et al. (2020). All dinoflagellate cyst taxa identified in this study are shown in Table 2, where they have been grouped according to the nutrition strategy of the motile stage: cysts produced by heterotrophic dinoflagellates ("heterotrophic cysts" onwards) and cysts produced by autotrophic dinoflagellates ("autotrophic cysts" onwards). The latter are probably all photo-mixotrophs, many of which are obligate phototrophs (Jeong et al., 2005; Flynn et al., 2019). Since this study dealt with living dinoflagellate cysts, the motile-stage based name (biological name) was used preferentially —when the cyst-theca relationship is well established and the vegetative stage known— always adding "cyst of" before to indicate that we are referring to the resting stage (cyst). When the vegetative stage was not clear or unknown, or when more than one cyst morphotype was related to a single motile species, the cyst-based name (paleontological name) was used instead.

TABLE 2 Dinoflagellate cyst taxa identified in this study with their corresponding motile cell names (following Zonneveld and Pospelova, 2015; van Nieuwenhove et al., 2020; Gu et al., 2021).

Heterotrophic taxa		Autotrophic taxa	
Cyst name	Motile cell	Cyst name	Motile cell
Cysts of *Archaeperidinium constrictum*	*Archaeperidinium constrictum*	*Alex*-type	Unknown
Brigantedinium sp.	*Protoperidinium* sp.	Cysts of *Gymnodinium catenatum*	*Gymnodinium catenatum*
Brigantedinium cariacoense	*P. avellana*	Cysts of *Gymnodinium microreticulatum* (<30 *mm* diameter)	*Gymnodinium microreticulatum*
Diplopsalis-type	Diplopsalid group	Cysts of *Gymnodinium nolleri/microreticulatum* (30–40 mm diameter, according to Amorim et al., 2002)	*Gymnodinium nolleri/microreticulatum*
Dubridinium caperatum	*Preperidinium meunieri*	*Impaginidium* sp.	Probably *Gonyaulax* sp.
Dubridinium sp.	Unknown	*Impaginidium aculeatum**	Unknown
*Echinidinium granulatum/delicatum**	Unknown (probably Protoperidinoid group)	*Lingulodinium machaerophorum*	*Lingulodinium polyedra*
Echinidinium transparantum/zonneveldiae	Unknown (probably Protoperidinoid group)	*Operculodinium centrocarpum*	*Protoceratium reticulatum*
Islandinium minutum	*Islandinium minutum*	Cysts of *Scrippsiella* cf. *trochoidea*	*Scrippsiella* cf. *trochoidea*
Cysts of *Lejeunecysta oliva**	Probably *Proptoperidinium* sp.	*Spiniferites* sp.	*Gonyaulax* sp.
Cysts of cf. *Lejeunecysta sabrina*	Probably *Proptoperidinium* sp.	*Spiniferites bentorii*	*Gonyaulax nezaniae*
Cysts of *Polykrikos kofoidii*	*Polykrikos kofoidii*	*Spiniferites delicatus/ristingensis**	*Gonyaulax* sp./*portimonensis*
Cysts of *Protoperidinium americanum*	*Protoperidinium americanum*	*Spiniferites membranaceus*	*Gonyaulax membranacea*
Cysts of *Protoperidinium monospinum*	*Protoperidinium monospinum*	*Spiniferites mirabilis/hyperacanthus*	*Gonyaulax spinifera* group/ *G. whaseongensis*
Cysts of *Protoperidinium stellatum**	*Protoperidinium stellatum*	*Spiniferites* cf. *ramosus*	*Gonyaulax* cf. *spinifera*
Quinquecuspis concreta	*Protoperidinium leonis*	*Thoracosphaera* sp.	cf. *Thoracosphaera* sp.
Selenopemphix nephroides	*Protoperidinium subinerme*		
Selenopemphix quanta	*Protoperidinium conicum*		
Trinovantedinium applanatum	*Protoperidinium shangaiense*		
Unidentifiable (brown) peridinoid cysts	Probably *Protoperidinium* sp.		
Unidentifiable RBC (round brown cysts)	Protoperidinoid?		
Unidentifiable SBC (spiny brown cysts)	Protoperidinoid?		
SBC-type 1	Unknown		
Votadinium cf. *concavum/rhomboideum* (sensu Gurdebeke et al., 2019)	Unidentified		
Votadinium calvum (sensu Gurdebeke et al., 2019)	*Protoperidinium latidorsale*		
Votadinium sp.	*Protoperidinium* sp.		
Xandarodinium xanthum	*Protoperidinium divaricatum*		

Taxa with an asterisk (*) were detected only in sediments. The underlined taxa correspond to cysts with a calcareous wall (Alex-type is included since it is likely to correspond to the organic inner membrane of taxa with calcareous cysts, whose external (calcareus) wall may have been lost after treatment with SPT, see: Amorim, 2001).

Cyst incubation experiments started in January 2020 and lasted until March 2020. Single full cysts were isolated by micropipette under the inverted light microscope (Olympus IX70) and washed in filtered sterilized seawater from the sampling site, before being transferred to 4-well culture plates (Nunclon-^{TM} Delta surface, Thermo Scientific cat n° 176740), each with 1 ml of the same seawater. Cysts were incubated at 19°C under a 12:12h light/dark cycle at a photon flux density of 100 µmol photons m^{-2} s^{-1} (Anderson, 1980; Montresor and Marino, 1996; Amorim et al., 2002). Cysts were checked daily for germination.

3.5 Lagrangian model

In order to understand the oceanographic conditions associated with the period of the fieldwork reported in this study, a numerical modelling configuration was used. We used an implementation of CROCO (V1.0) numerical model of the circulation in the region, forced by realistic winds and heat fluxes, based on configurations similar to the ones reported and validated by Cordeiro et al. (2021). The outputs were hydrographic fields (temperature, salinity and density), and currents (u, zonal, and v, meridional current), with a horizontal resolution of about 500 m, saved every 2 hours. Those outputs were used to set up a Lagrangian framework using ROFF (Carr et al., 2008) in a similar way to Nolasco et al. (2018), consisting of particles along the main section of observations, at the time of the measurements reported (14th and 19th September) from the coastal station (#1, ~15 m depth) to the offshore one (#10, ~150m depth). The particles were initially located near the bottom at different depths: 1, 5 and 10 meters above the bottom (mab) and were tracked backwards in time to assess their origin in the previous 10 days. Buoyancy effects were not considered in this study assuming that the cysts were neutral. Although sinking of the cysts was modelled and thoroughly discussed at the global scale (Nooteboom et al., 2019), we were interested in modelling the origin of the cysts at the spatial scale of the continental shelf and time scale of one week.

4 Results

4.1 Water column environmental properties and bottom nepheloid layer during cyst sampling

During the sampling campaign (14th-19th of September 2019), the study area was still influenced by upwelling, as reflected by the occurrence of colder waters with higher Chl-*a* concentrations (enhanced primary productivity) near the coast (Figures 2A, B). The CTD profiles represented a transition from upwelling to relaxation conditions (Figures 3A, B). On 14th September 2019, minimum temperatures and a zone of divergence near the coast (~5 km to the coastline) were observed (transect 1, Figure 3A). In contrast, five days later (19th September 2019) warmer waters from the slope expanded, spread throughout the shelf and reached the coast (transect 2, Figure 3B). In both transects a well-defined thermocline was observed. The thermocline varied with depth due to the internal wave propagation. The SSC data collected during the cruise showed low concentration values (<2.0 mg/l). The BNL mainly developed over the outer shelf muddy deposits (IH- Chart SED 2), reaching 20-30 m in height. On 19th of September it intensified at increased depths (Figure 3B). In the outer shelf, the fixed CTD station (#7) showed a similar oceanographic regime, with a well-developed thermocline at a depth that shifted throughout the observation periods in days 16th (~8h, 31 CTD stations) and 18th of September (~5h, 15 CTD stations). Vertical displacements of the thermocline of about 20-30 m of magnitude were particularly relevant (see the 0.5 mg/l isoline in the SSC profile), and were associated with the passage of internal waves (Figure 4).

4.2 Dinoflagellate cyst records

4.2.1 Notes on cyst identification

Alex-type refers to spherical cysts with relatively thick walls and no processes, always bearing cell contents and a red to yellowish accumulation body. They resembled some resting cysts of *Alexandrium minutum* and other *Alexandrium* species (Bolch et al., 1991; Bravo et al., 2006). These cysts were in general more abundant in sediments than in water samples. As the use of sodium polytungstate can decalcify cysts with calcareous walls (Bolch, 1997; Amorim, 2001), some *Alex*-type cysts found in sediments (e.g., Image 20, Plate 1) could actually correspond to calcareous cysts that had lost their mineral outer wall. Therefore, calcareous cysts could be underrepresented in the sediment samples analyzed in this study.

Round brown cysts that differed from cysts of *Brigantedinium* spp. (cysts of *Protoperidinium* spp.) in being generally smaller in diameter (<30 µm) and lighter in color (e.g., images 1 and 2, Plate 1) and not showing archeopyle were included in the group of RBC (Table 2). They also differed from cysts of *Dubridinium* spp. (cysts of Diplopsalioideae) (e.g., Image 3, Plate 1) in being thinner-walled and not dorso-ventrally compressed (Mudie et al., 2017). Some RBC showed an elongated, split-like archeopyle and were therefore classified as *Diplopsalis*-type (Image, Plate 1). These cysts were added to the RBC group for graphical representation and statistical analyses.

The group of SBC (Table 2) generally included unidentifiable small spiny brown cysts. These cysts were generally small and the process shape and tip, which are key for the cyst species identification (see Radi et al., 2013), were difficult to observe in detail because they often appeared broken or attached to organic detritus. A few of these SBC could be identified and photographed, as is the case of *Protoperidinium monospinum* (Images 10 and 11, Plate 1), which was abundant in some BNL samples. Other cysts that could not be identified and quantified in all samples and therefore were added to the SBC group for graphical representation and statistical purposes were: cysts of *Archaeperidinium constrictum* (images 8 and 9, Plate 1), *Islandinium minutum* (no images shown), *Echinidinium transparantum/zonneveldiae* (images 15 and 16, Plate 1), *Echinidinium granulatum/delicatum* (found only in sediments, no images shown) and SBC-type 1 (images 13-14, Plate 1). SBC-type 1 is a small cyst (~15 µm), pale brown and with short (<3.5 µm) processes. It closely resembled *Islandinium brevispinosum* (Pospelova

and Head, 2002) in having short, solid and numerous processes. However, it differed from *I. brevispinosum* in that the processes were less densely arranged and the wall was apparently granulated.

4.2.2 Dinoflagellate cyst distribution in the BNL

A total of 30 dinoflagellate cyst types were identified in the BNL samples, excluding the unidentifiable round brown cysts (RBC), spiny brown cysts (SBC), and other non-identified species (Table 2). Most were organic-walled, although calcareous cysts consistently occurred (at low abundances). Considering both samples from the land-sea transects (Figure 5) and temporal series (Figure 6), the most abundant calcareous cyst type was *Scrippsiella* cf. *trochoidea* (Image 19, Plate 1) with percentages ranging 0-6.2% of the total dinoflagellate cyst sum. Among all cysts, the most abundant type was heterotrophic spiny brown cysts (SBC), with percentages ranging 10.4-93.3% of the total cyst sum, except in sample collected on 14th of September at station #1, where no SBC were observed (Figure 5). In this sample, abundances of cysts of *Protoperidinium conicum* (19.7%) and *Votadinium* spp. (12.4%) increased. Other abundant cyst taxa in the BNL off Figueira da Foz were *Brigantedinium* sp. (0-6.1%), cysts of *Protoperidinium subinerme* (0-15.9%), *Dubridinium* sp. (0-51.8%) and round brown cysts or RBC, which included *Diplopsalis*-type (2.1-37%), all heterotrophic taxa. Among autotrophic taxa, the most abundant cysts along the land-sea transects (Figure 5) were *Spiniferites* cf. *ramosus* (0-32.2%) (Image 17, Plate 1) and cysts of *Protoceratium reticulatum* (0.4-18.9%) (Image 18, Plate 1). In the time-series records studied at station #7, the presence of empty cysts of *Gymnodinim* spp. (0-5.6%) was also notable (Figure 6).

The spatial distribution of dinoflagellate cyst assemblages in the BNL along the two transects studied (14th and 19th September) generally showed great differences between coastal (<100 m depth and at<25 km from the coast) and more offshore stations (>100 m depth and >25 km from the coast) (Figures 5A, B). Total cyst concentrations generally ranged 37-137 cysts/l, but they notably decreased in offshore stations #7, #9 and #10 (3-26 cysts/l). The highest values (115-137 cysts/l) were recorded at stations #3 and #5 (Figure 5B), at ~50 and ~80 m depth respectively (Figure 1C). Full

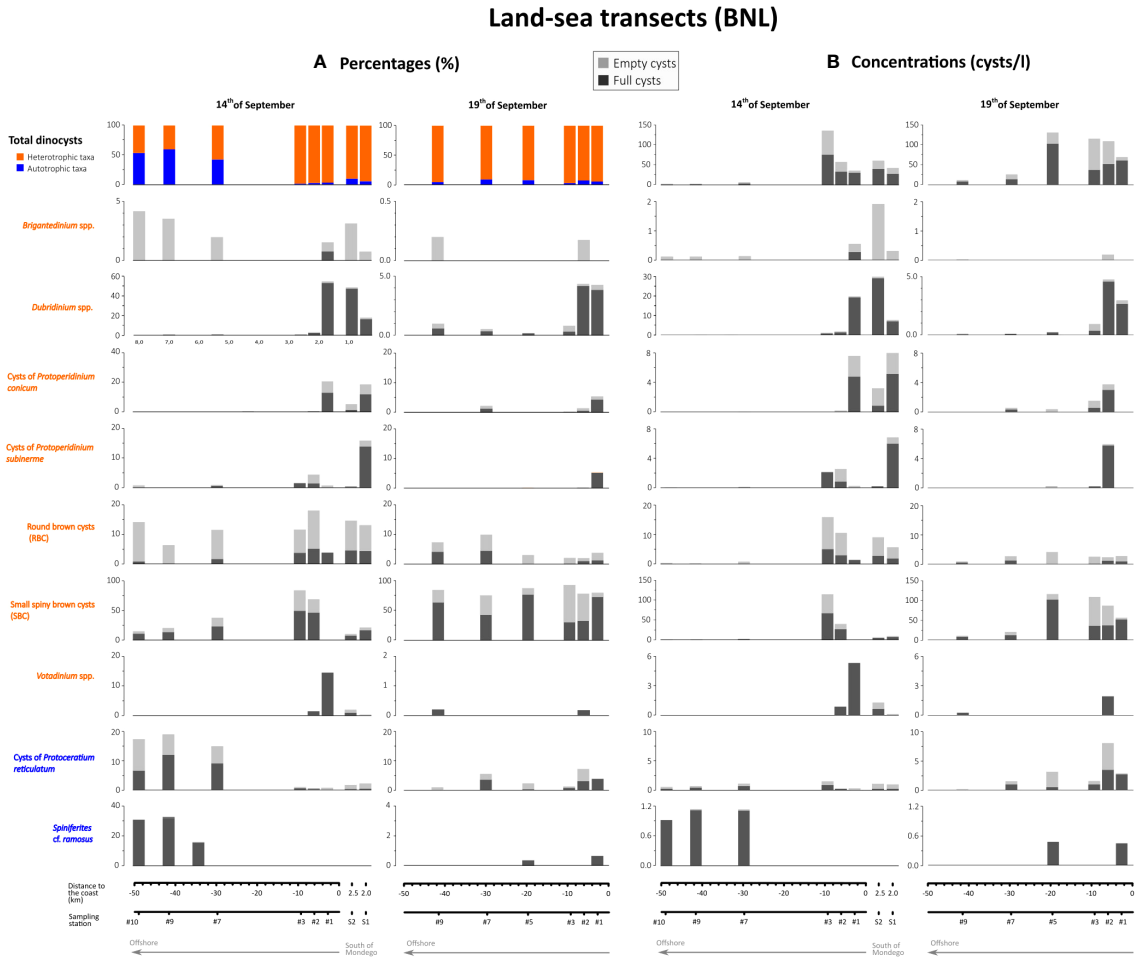

FIGURE 5
Relative **(A)** and absolute **(B)** abundances of dinoflagellate cysts observed in the BNL along the two land-sea transects studied (14th and 19th September 2019) off Figueira da Foz. Along the horizontal axis, sampling stations were ordinated following and inshore-offshore gradient (from right to left), except for stations #S1 and #S2 sampled on 14th September south of the Mondego Cape (Figure 1B). Only the most abundant cyst types are shown. *Votadinium* sp., *V. calvum* and *V.* cf. *concavum* (sensu Gurdebeke et al., 2019) were grouped into *Votadinium* spp. Note the different scales of the abundance axes between different cyst taxa.

10.3389/fmars.2023.1270343

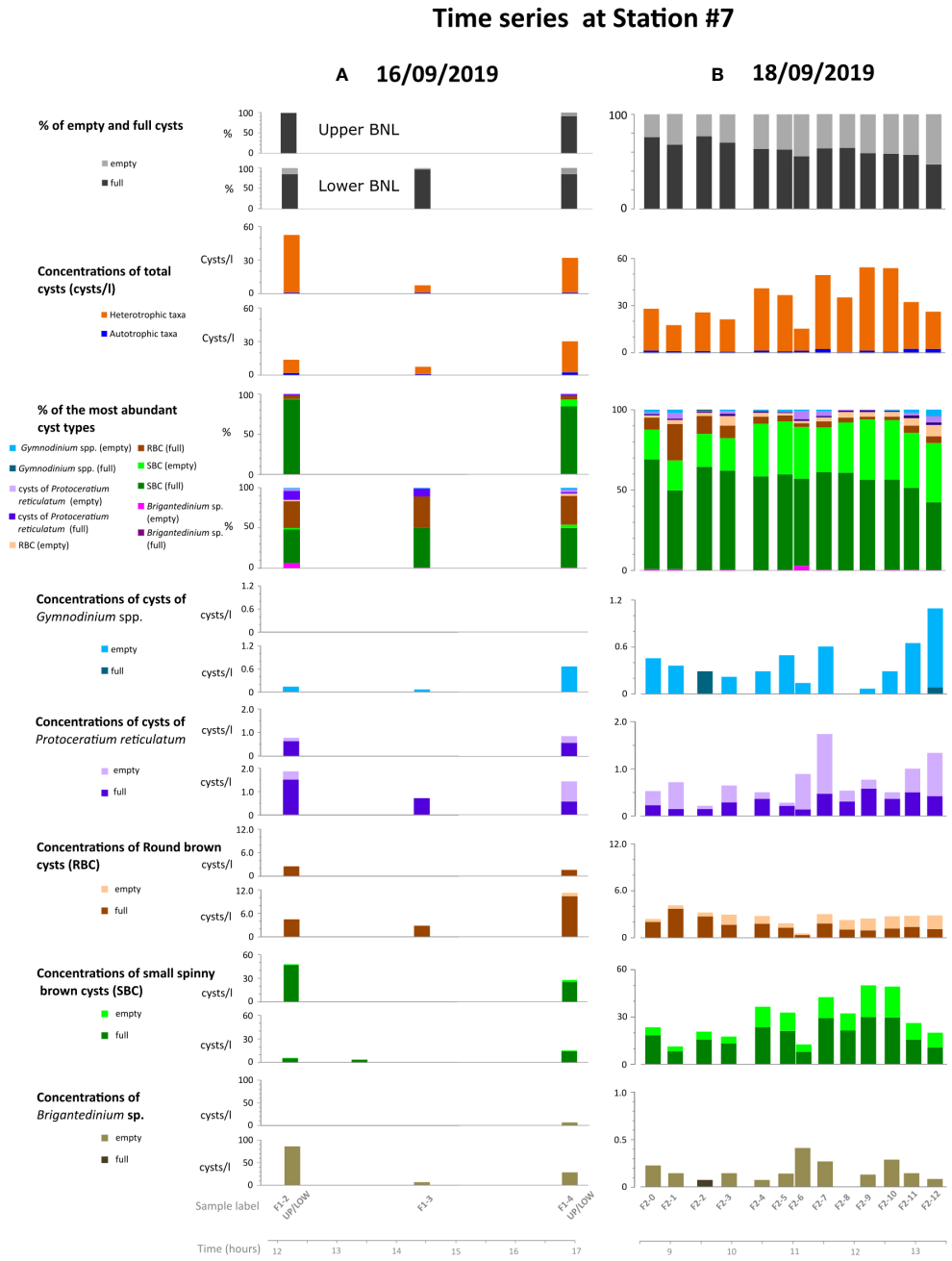

FIGURE 6
Temporal distribution of dinoflagellate cyst records during part of the days 16th **(A)** and 18th **(B)** of September 2019 at station #7. Only the most abundant cyst types are shown. Note the different scales of the abundance axes between different cyst taxa.

cysts generally dominated cyst assemblages, showing >50% of the total cyst sum in most samples (Figure 5A). Empty cysts increased in samples collected on 19th of September at stations #2 (52.1%) and #3 (67.1%). Heterotrophic cysts represented >80% of the total cyst sum in most samples, except for those collected on the 14th of September at offshore sites (stations #7, #9 and #10), where autotrophic cysts increased (42-60%). Here, both percentages and concentrations of full cysts of *S.* cf. *ramosus* (Image 17, Plate 1) notably increased (Figure 5B). From the 14th to the 19th of September, concentrations (and percentages) of most taxa generally decreased in all stations, except for cysts of *P. reticulatum* and SBC, whose concentrations increased over time, notably at inshore stations. Concentrations of SBC peaked on the 19th of September at stations #3 (108 cysts/l) and #5 (115 cysts/l), and cysts of *P. reticulatum* in 2# (11 cysts/l) (Figure 5B).

Temporal variation of cyst records in the BNL on the 16th (between 12:14 and 16:57 hours) and 18th of September (between 8:41 and 13:16 h) at station #7 is shown in Figure 6. Total cyst concentrations varied between 8 and 55 cysts/l. The highest values (54-55 cysts/l) were recorded on the 18th of September, in samples F2-9 and F2-10, collected at 12:13 h and 12:36 h, respectively (Figure 6B). After this, cyst concentrations in the BNL decreased

(samples F2-11 and F-12), coinciding with a lowering of the thermocline recorded at ~12:45 h (Figure 4B). Full cysts represented >85% in the cyst samples obtained on the 16th (Figure 6A); these proportions decreased (48-77%) on the 18th (Figure 6B). Proportions of empty cysts increased with depth on day 16th (they are higher in the lower than in the upper BNL) and over time on the 18th, reaching the highest value (52.5%) in the last sample (F2-12) collected at 13:16 h. During both days, cyst records were dominated by heterotrophic cysts (86-98%), SBC being the dominant cyst type (40.9-93.3%). RBC was also abundant in time-series cyst records (4.7-37.6%). On the 18th, proportions and concentrations of empty SBC and RBC increased substantially. Regarding *Gymnodinium* spp. (which included *G. catenatum* and a few cysts of *G. cf. microreticulatum*), most cysts were empty (0-4.1%) (Figures 6A, B).

4.2.3 Dinoflagellate cyst distribution above the BNL

Mean concentrations per depth level of total dinoflagellate cysts, small spiny brown cysts (SBC) and cysts of *Protoceratium*

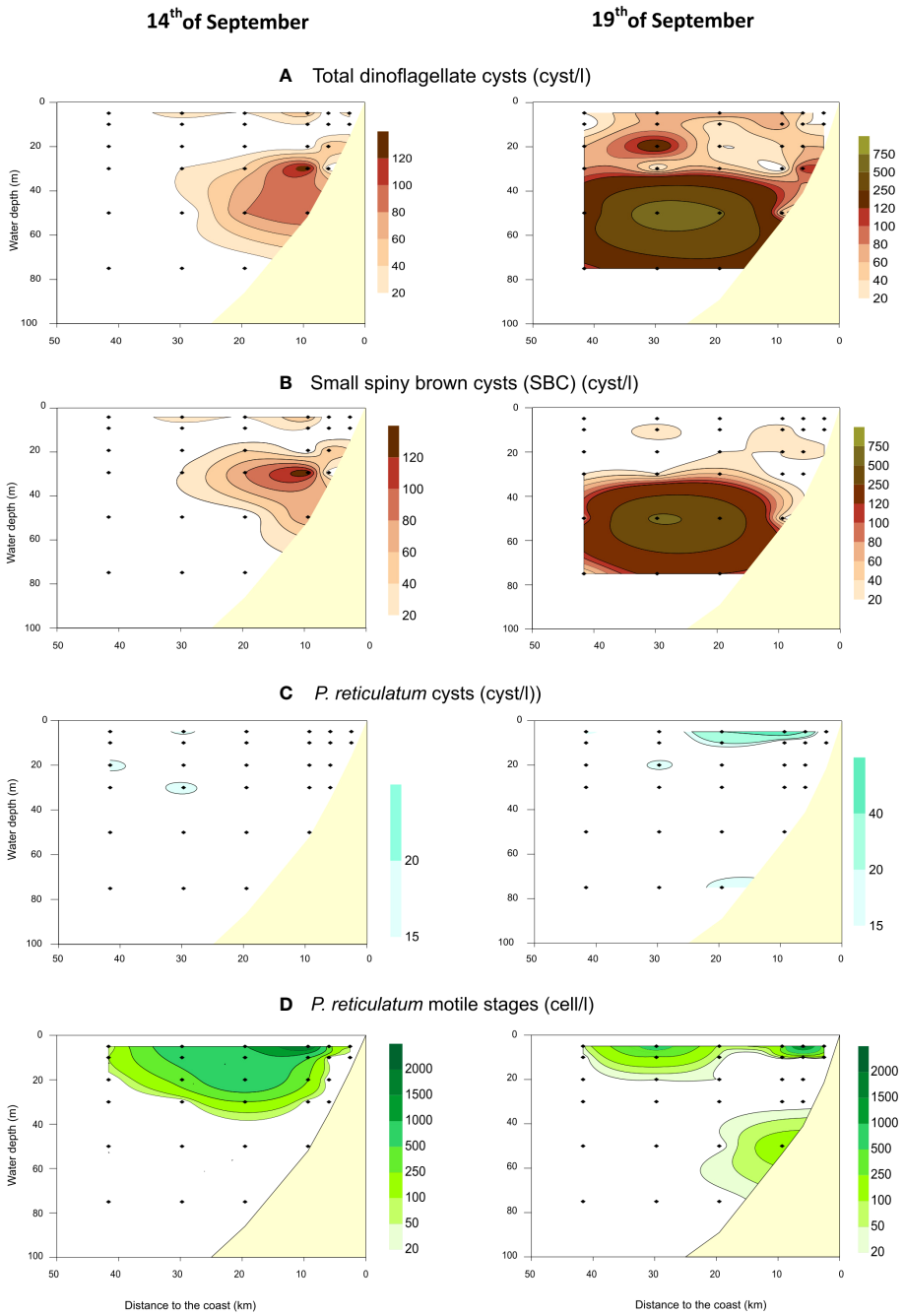

FIGURE 7
Vertical and horizontal distributions of mean total cysts concentrations **(A)**, small spiny brown cysts **(B)** and cysts **(C)** and cells **(D)** of *Protoceratium reticulatum* (Moita et al., 2022) along the two land-sea transects sampled on 14th and 19th September 2019 off Figueira da Foz.

reticulatum are shown in Figures 7A–C. Other cyst taxa identified (but not quantified in all water samples above the BNL) were: *Scrippsiella* sp., *Diplopsalis*-type, cysts of *Protoperidinium conicum* and cysts of *Lingulodinium polyedra*. Total mean cyst concentrations were very variable according to depth and distance to the coast. They ranged between 0 and 140 cysts/l on the 14th of September, and increased on the 19th, with values ranging between 0 and 800 cysts/l (Figure 7A). All the observed cysts had cell contents and were generally distributed above the base of the pycnocline, i.e., ~40-50 m depth (Figures 3, 7). Likewise in the BNL, small spiny brown cysts (SBC) were generally the most abundant cysts. SBC were already abundant (<140 cysts/l) on the 14th of September at ~30 m depth, in mid-depth stations (stations #3 and #5). On the 19th of September, SBC concentrations increased (<800 cysts/l) at greater depths (~50 m depth) in more offshore stations (Figure 7B). The cyst distribution of *P. reticulatum* was very different from that of SBC, with lower concentrations (<60 cysts/l) and showing a distribution center in more surficial waters (Figure 7C). On 14th of September,<20 cysts/l were recorded in offshore stations. Mean concentrations increased on 19th of September at the surface in more coastal stations (Figure 7C). Spatial and temporal mismatches between the distribution of cysts (Figure 7C) and planktonic stages (Figure 7D) of *P. reticulatum* could be observed. On the 14th, cysts of *P. reticulatum* were found more offshore than the cell distribution center. Moreover, cyst concentrations increased over time; reaching the highest concentrations on the 19th of September in mid-depth stations (Figure 7C). In contrast, on the 19th the cell bloom was already decreasing and getting patchier, with the highest cell concentrations observed in the 2nd inner shore station and 30 km offshore (Figure 7D). The bloom never exceeded 200 cells/l at the innermost station.

4.2.4 Sediment trap cyst record

The sediment trap recorded the vertical cyst rain from the 7th to the 19th of September at ~90 m depth at station #7 (Figure 2). Empty (48.3%) and full (51.7%) cysts occurred in almost equal proportion (Figure 8). Total cyst flux was 38,897 cysts/m^2/day. As in water samples, heterotrophic cysts were dominant (79.4%) and SBC was the most abundant cyst type (72.8% of the total cyst sum). Among autotrophic cysts, cysts of *Protoceratium reticulatum* were the most abundant type (16.2% of the total cyst assemblage). This cyst record was similar to that obtained in the BNL on the 19th of September in the same station (sample T2-7) (Figure 5). In this sample, a similar empty/full ratio (46.2%/53.8%) was recorded, as well as relatively high proportions of heterotrophic cysts (91.1%), SBC (76.1%) and cysts of the autotrophic *P. reticulatum* (5.6%) (Figure 5). On the other hand, in the sediment trap cyst diversity (especially of autotrophic taxa) was higher than in sample T2-7. In the sediment trap, higher cyst abundances of clear cysts —such as cysts of *Spiniferites* spp., *Scrippsiella* cf. *trochoidea* and *P. reticulatum*— were recorded, as well as the occurrence of *Lingulodinium polyedra*, that was absent from T2-7 record.

4.2.5 Dinoflagellate cyst distribution in surface sediments

A total of 35 dinoflagellate cyst types were identified in sediments, excluding the unidentifiable round brown cysts (RBC), spiny brown cysts (SBC), and other non-identified species (Table 2). In contrast to BNL samples, autotrophic cysts (36.5-78.4%) were

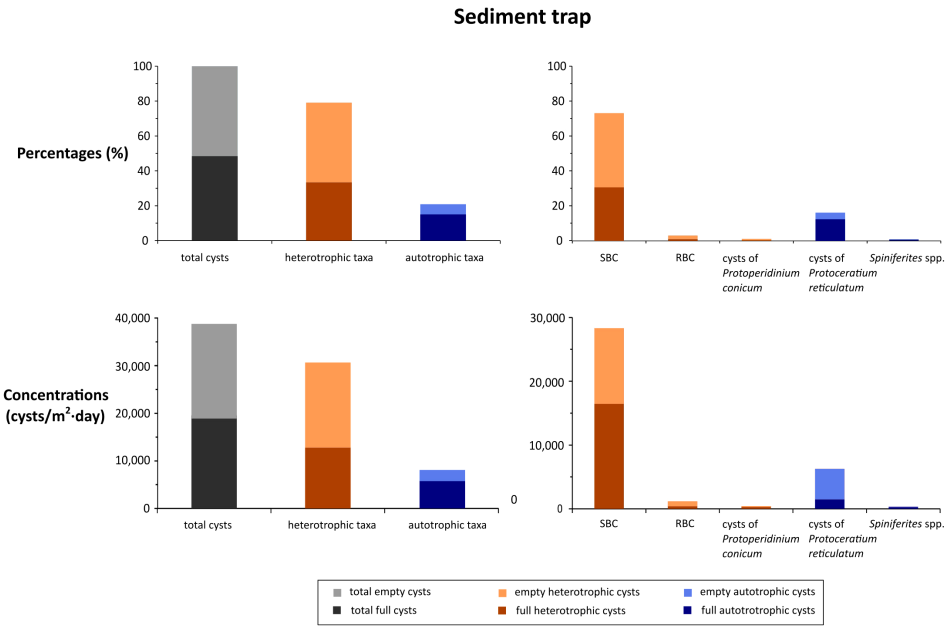

FIGURE 8
Sediment trap dinoflagellate cyst record. Cyst percentages and fluxes in the cyst rain from 7th to 19th September 2019 at station #7. Only selected cyst types are shown.

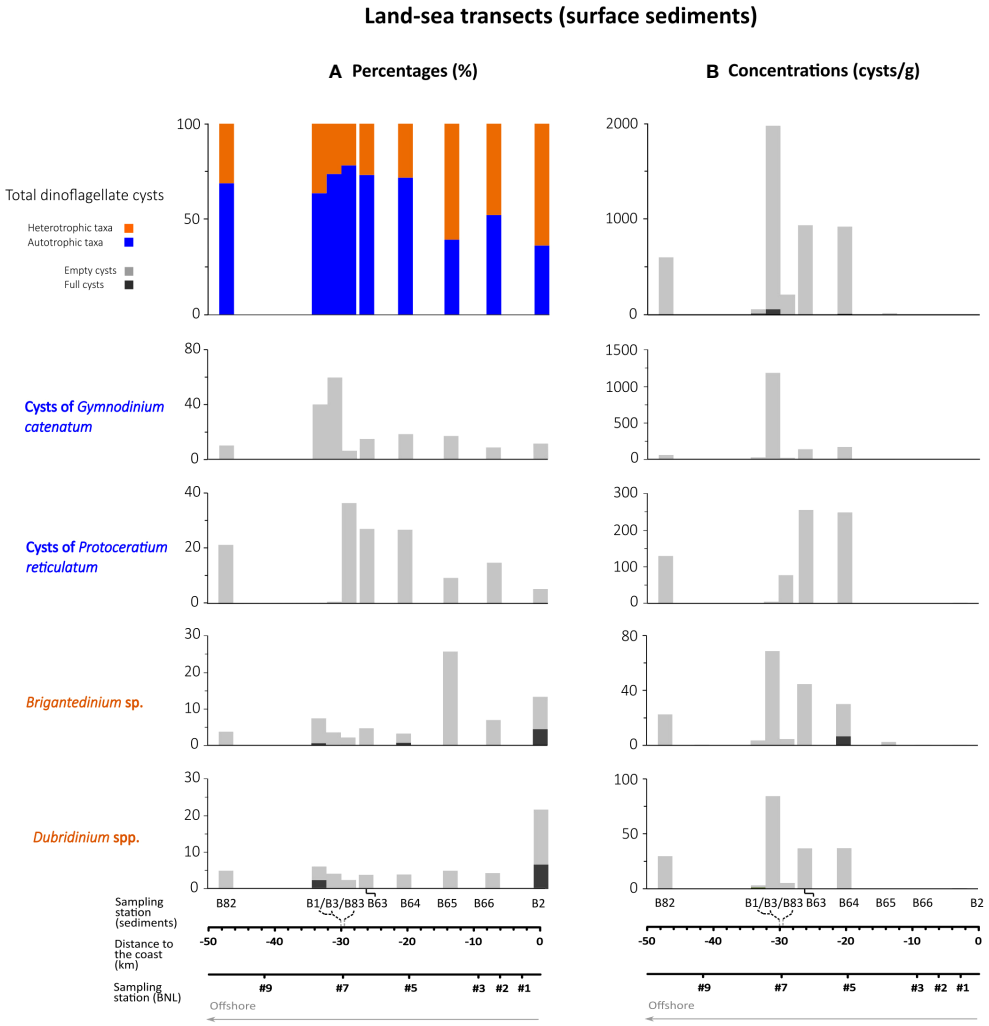

FIGURE 9
Dinoflagellate cyst percentages **(A)** and concentrations **(B)** in the sediment samples collected along the land-sea (right to left in the x-axis) transect off Figueira da Foz. Only the most abundant types are shown. Note that samples B3, B1 and B83 were collected at practically the same location.

dominant in cyst records from sediments; except for samples B65 and B2 where autotrophic cysts were<50% of the total cyst sum (Figure 9). Heterotrophic cyst proportions increased (63.5%), south of Cape Mondego, in the shallowest station at the Mondego River's mouth, sample B2 (Figure 1B); however, in this sample, only 52 cysts were counted. Along the land-sea transect, cyst concentrations in surface sediments ranged between 3 and 2002 cysts/g, drastically decreasing inshore (<10 cysts/g). This contrasts to cyst distribution in the BNL, where concentrations were substantially higher in shallow stations (<100 m depth) and decreased offshore (Figure 5). Another difference with water samples was that in sediments, cyst records were dominated by empty cysts (>63.5%). The most abundant cyst taxa in surface sediments (by decreasing order of maximum percentages) were: cysts of *Gymnodinium catenatum*, cysts of *Protoceratium reticulatum*, *Brigantedinium* sp. and *Dubridinium* spp. Cyst concentrations notably increased in sample B3, where cysts of *G. catenatum* were the most abundant type (1180 cysts/g). In addition to concentrations, one can also observe outstanding differences between the cyst records of samples B1, B3 and B83, samples that were tentatively collected in the same location as station #7 (although at different times) (Figure 1B; Table 1). Percentages of *G. catenatum* were much higher in samples B1 and B3 (collected in September 2019) than in sample B83 (March 2019). Moreover, sample B3 showed much lower percentages of cysts of *P. reticulatum* than samples B1 and B83 (Figure 9).

4.2.6 Clustering and cyst record comparison

Cluster analysis grouped the samples (from the BNL, sediment trap and sediments) according to their similarities in dinoflagellate cyst composition (Figure 10). Samples collected in the BNL on the 14th of September at the most offshore stations (>100 m depth) and those from the most inshore sites (<30 m depth) significantly differed from those obtained the same day at mid-depths, all samples collected on 19th of September and the sediment trap cyst record. Offshore samples collected on the 14th (T1-7, T1-9 and T1-10, blue circles in Figure 10) were similar to sediment cyst records (blue squares, Figure 10), while inshore samples (T1-1, S1

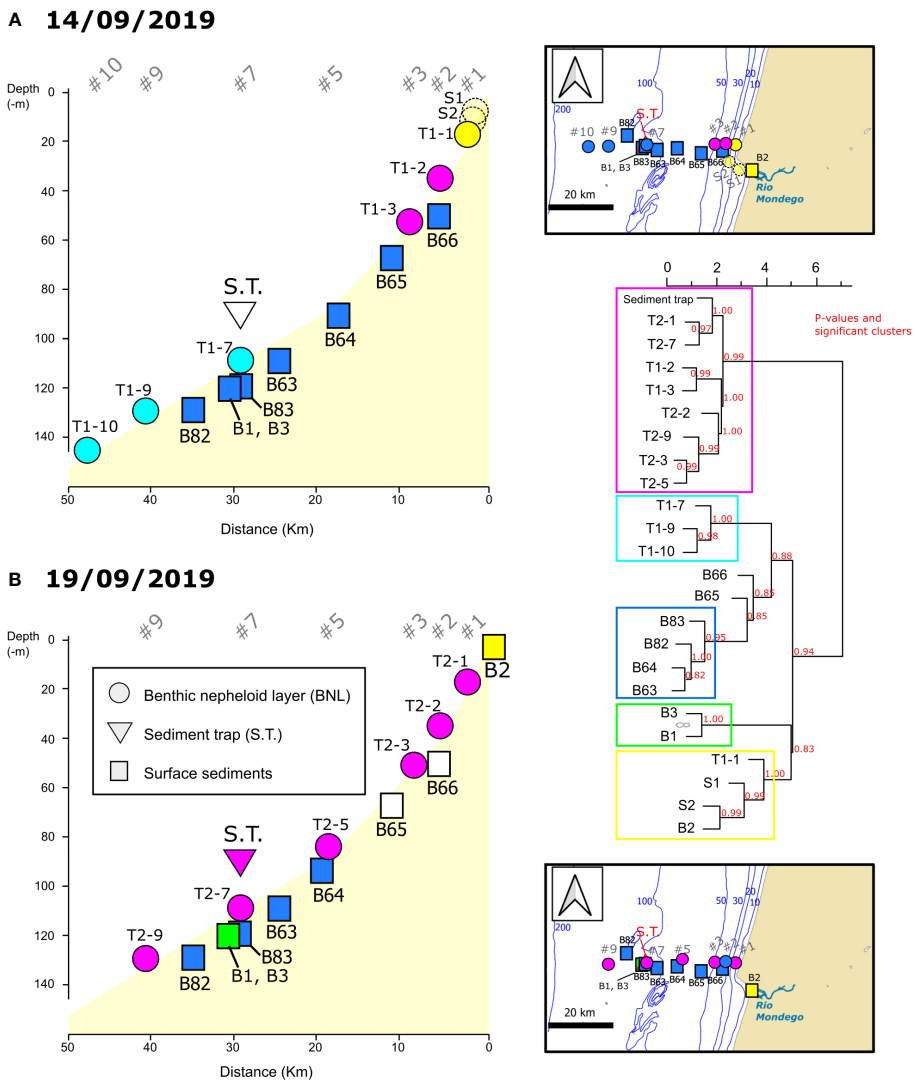

FIGURE 10
Cluster analysis performed on square-root transformed percentage dinoflagellate cyst data of samples collected in the BNL on 14th **(A)** and 19th **(B)** of September 2019, sediment trap and surface sediments along the land-sea transect off Figueira da Foz. The resulting dendrogram showing the classification of samples and p-values is presented on the right. Samples (labelled as in Table 1) were grouped in 5 main clusters (different colors) according to differences in cyst composition (and clusters' significance).

and S2, yellow circles in Figure 10) were more similar to the sediment cyst record obtained in the harbor area at the Mondego River's mouth (yellow square in Figure 10). Note that in this sample only 52 cysts were counted, as it was constituted by coarse sediments poor in organic content; therefore, the similarities detected by clustering should be analyzed with caution. The other BNL samples were similar to the sediment trap cyst record (in pink, Figure 10) and substantially differed from sediment cyst records.

In accordance with clustering results, the autotrophic cysts of *Gymnodinium catenatum* and *Lingulodinium polyedra* were especially abundant in sediments (6.3-58.9% and 0-18.4% respectively), while in BNL and sediment trap samples these taxa were scarce (0-1.3% and 0-0.8%, respectively). Some cysts were found in sediments but not retrieved from water samples: *Echinidinium granulatum/delicatum*, cysts of *Lejeunecysta oliva*, cysts of *Protoperidinium stellatum, Impaginidium aculeatum* and *Spiniferites delicatus/ristingensis* (with an asterisk in Table 2). The BNL samples T1-7, T1-9 and T1-10 (offshore stations sampled on the 14th of September) were more similar to sediment cyst records than to other BNL because they had greater abundances of autotrophic taxa mainly: cysts of *Lingulodinium polyedra*, *Protoceratium reticulatum* and *Spiniferites* spp. Moreover, the abundances of SBC were significantly lower than in other BNL samples. On the other hand, samples T1-1, S1, S2 and B2 (inshore stations sampled on the 14th of September) had in common relatively high percentages of *Brigantedinium* spp., *Dubridinium* spp. and cysts of *Protoperidinium conicum*, and low proportions of SBC, if compared with other BNL samples (Figures 5, 9).

4.2.7 Excystment experiments

A total of 63 cysts with apparently viable cell contents from the BNL were isolated and incubated for excystment in the laboratory.

TABLE 3 Summary of the results obtained from isolation and germination experiments.

Cyst types that excysted in the laboratory	Number of isolated cysts	N (number of germinated cysts)	Germination time/Mean germination time (days)	Range (days)
Alex-type	2	1	6	-
Protoceratium reticulatum	5	3	5.6	3-7
Clear round cyst	8	3	20.3	6-29
RBC	18	4	12.5	1-40
Scripsiella cf. *trochoidea*	1	1	3	-
Small mucous cyst	1	1	14	-
SBC (*P. monospinum* included)	25	6	8.5	4-19
Spiniferites cf. *ramosus*	3	0	–	-
	63	**19**		
	Total isolated cysts	**Total germinated cysts**		

Of these, 17 cysts (27%) were observed to germinate in the laboratory (Table 3). Initially, the purpose of these experiments was to identify by single-cell PCR the cysts with unknown affinity; however, these experiments were unsuccessful. Despite this, cyst incubations helped in assessing the viability of full cysts and determining the germination times of various cyst types. Given the time that mediated between sample collection and isolation, all cysts were already at least 4 months old. Isolated taxa included: *Alex*-type, unknown spiny brown cysts (SBC), round brown cysts (RBC), clear round cysts, small mucous cysts, cysts of *Protoperidinium monospinum*, *Scripsiella* cf. *trochoidea*, *Spiniferites* cf. *ramosus* and cysts of *P. reticulatum*. The mean germination times under the selected incubation conditions are shown in Table 3. In the case of SBC, germination times varied between 4 and 19 days. Among them, one cyst could be identified as *P. monospinum* and took 5 days to germinate. In the case of RBC, germination times were very variable (1-40 days) suggesting differences in maturation and germination physiology of the different species.

4.3 Modelled cyst trajectories in the BNL

The Lagrangian particle-tracking model simulated the cyst trajectories 5 and 10 days before reaching the land-sea transects sampled on the 14th and 19th of September (Figures 11A–F). Results predicted a different behavior of particles between inshore (<100 m) and offshore (>100 m) sites. At coastal stations, the origin of the cysts recorded at the Figueira da Foz transect is located to the north, indicating equatorward transport associated with the upwelling jet induced by northerly winds in the previous days. In contrast, at offshore stations, cysts were advected from the south, possibly associated with the Iberian poleward current of the outer shelf and upper slope. Moreover, the model predicted an intensification of alongshore equatorward velocities for the cysts located near the coast (Figures 11A, D). Alongshore transport was observed to decrease over time, reaching minimal values between days 14th and 19th when reconstructed cyst trajectories were the shortest (red and black symbols in Figures 11D, F). This agrees with the presence of a maximum of northerly (upwelling favorable) winds observed on days 11th-12th of September, the wind weakening from the 12th-16th and the calm conditions until the 19th September (Figure 2). The model also predicted that vertical cyst transport was low overall, being mostly restricted to the BNL (Figures 11B, E). This vertical contribution was more intense at offshore sites than inshore. The particles coming from the north were observed to be advected in the BNL in the presence of an inshore transport to the left of the equatorward jet according to the bottom Ekman dynamics, while the deeper particles (depth >100m) were slowly advected polewards from the south.

5 Discussion

5.1 Origin of dinoflagellate cysts in the BNL

Large abundances of full cysts observed in the BNL (Figures 5, 7) suggested that the main cyst source had a recent origin. This is supported by clustering since most cyst records were statistically similar to the sediment trap and very different to the sediment cyst records (Figure 10). Samples collected on 14th of September in the deeper stations (>100 m depth), i.e. samples T1-7, T1-9 and T1-10, were more similar to samples from the underlying sediments (Figure 10), which indicated significant local resuspension affecting the BNL cyst records. Moreover, the cyst records from the shallower stations (<30 m) sampled on the 14th of September, i.e. samples S1, S2 and T1-1, were grouped with the sample collected at the Mondego River's mouth (B2), which could suggest the influence of fluvial sediments. Surface sediments in the study area showed an increasing grain-size trend towards the coast, with coarser sands near the Mondego's River mouth (García-Moreiras et al., 2021). This is coherent with the proximity of these stations to

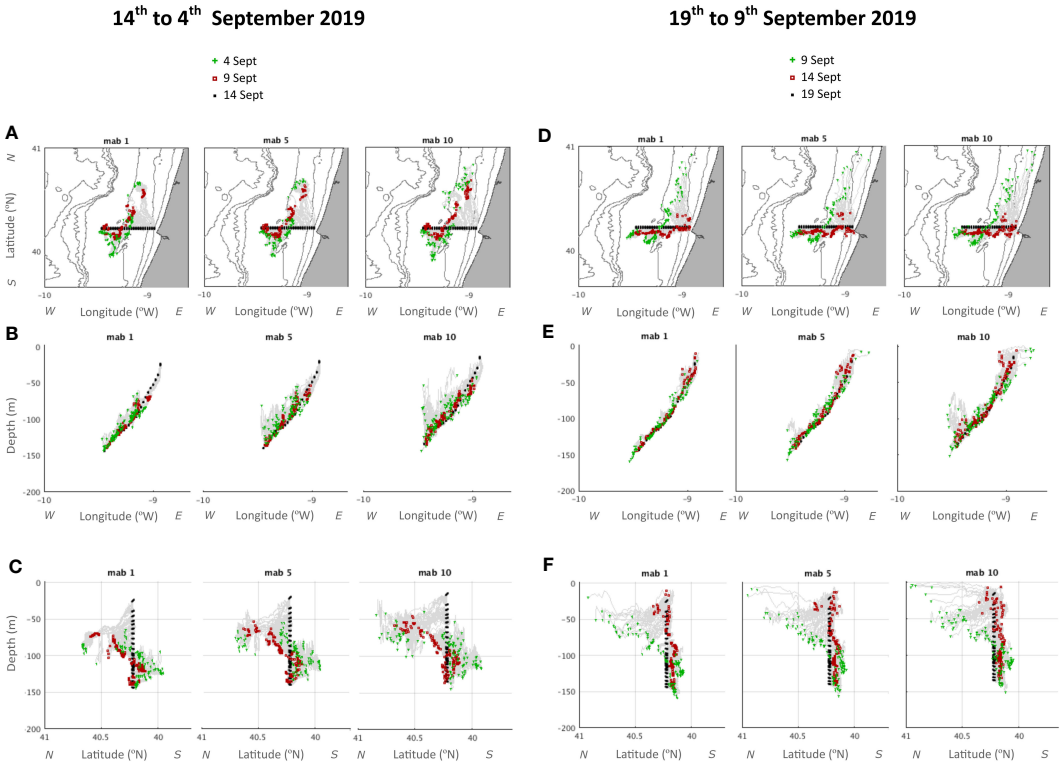

FIGURE 11
Trajectories of Lagrangian particle experiments simulating cysts, integrating backwards in time during 10 days from days 14th **(A-C)** and 19th September 2019 **(D-F)**. **(A, D)** represent the horizontal view from above (longitude-latitude) showing the trajectories of cysts at 1, 5 and 10 meters above the bottom (mab). **(B, E)** represent the same as **(A, B)** for a lateral longitude-depth slice view from the south of the same simulation. **(C, F)** represent lateral latitude-depth slice view from the west, for the 1, 5, and 10 mab initial releasing of simulated cysts. Isobaths 25,50,100,250,500,1000 and 2500 m are represented in **(A, D)**. The cyst's initial positions are represented in black dots, the paths in continuous grey lines, and the predicted positions 5 and 10 days before cyst sampling in red squares and green crosses, respectively.

the river mouth. However, considering that a very low cyst count (52 cysts) was obtained in this sample (B2), these results must be considered with caution.

Samples B1 and B3 resulted significantly different from other sediment samples, in terms of cyst composition (Figures 10, 11). Although samples B1 and B3 were obtained approximately at the same location as B83, this is not surprising, since the latter was collected 6 months before, in March 2019, and the other two samples in September 2019. These differences in cyst composition detected by clustering indicate that intra-annual variability in cyst production leaves an imprint in surface sediments (Figure 10).

The remaining cyst records in the BNL (samples T1-2 and T1-3 collected on the 14th September, and all the samples collected on the 19th) were very different from sediment records (Figure 10). This could be due to the occurrence of little sediment resuspension and to a stronger contribution from the cyst rain, that would make these BNL assemblages differ from those in bottom sediments. In general, our results indicate that the predominant physical (hydrodynamics regime) and biological (encystment and excystment) processes affecting cyst composition of the BNL changed relatively quickly, i.e., in only 5 days (Figure 10). A decrease in sediment resuspension over time would be consistent with changes in hydrodynamics (reduced turbulence) related to the upwelling relaxation (Ferreira Cordeiro et al., 2018).

The similarities observed between the BNL samples collected on 14th September at stations #2 and #3, all BNL samples obtained on 19th September and the sediment trap cyst record (Figure 10) supported that most cysts were closely related to the recent production in the water column (cyst rain). In particular, the sediment trap record (Figure 8) was rather similar to sample T2-7. For instance, both have similar heterotrophic/autotrophic cyst ratios (21%/79% in sediment trap and 9%/91% in sample T2-7) and empty/full cyst ratios (48%/52% and 46%/54%, respectively), as well as similar SBC percentages (~70% in both samples) (Figures 5, 9). Given the position of the sediment trap (-90 m), i.e., very close to the sampling point of T2-7 (-110 m), it could be possible that its cyst record was influenced by the BNL cyst content through upward vertical transport. However, the occurrence of stratified waters (Figure 4B), which agreed with little vertical contribution of particles near the bottom, as predicted by modelling results (Figures 11B, E), would have not favored upward vertical motions in the water column.

Consistent with the fact that little resuspension of bottom cysts might have affected the water-column cyst distribution off Figueira da Foz are the results recently obtained by Villacieros-Robineau et al. (2019) in a similar area further north from our study site, on the NW Iberian continental shelf. They detected little resuspension of the bottom sediments during the upwelling season on the inner

shelf. During this season the nepheloid layers were thinner and mainly composed of biogenic particles if compared to the downwelling season. Higher levels of bottom shear stress that caused strong resuspension of bottom material and thicker BNL occurred mainly during the downwelling season, due to higher storminess and more intense currents.

Further evidence supporting that a great part of the cysts in the BNL off Figueira da Foz come from recent encystment is that the spatial distribution pattern of cysts of *Protoceratium reticulatum* in the BNL along the transect was consistent with the distribution of motile stages in more surficial waters. The highest cyst concentrations generally coincided in space with peaks in cell abundances, i.e. at mid-depths on the 14th and at shallower sites on the 19th September (Figure 12A). Cyst concentrations in the BNL positively correlated with cell concentrations along the two land-sea transects (Figure 12B), indicating that these cysts in the BNL came from recent formation in the bloom that was developing in surface waters.

But what was the origin of empty cysts found in the BNL? Empty cysts could come from resuspension of older material or *in situ* germination. Previous studies indicated that particle distribution within the water column, and therefore the BNL structure, can be affected by the variability of internal waves and thermal stratification through local sediment resuspension (e.g., Oliveira et al., 2002; Thomsen et al., 2002; Gardner et al., 2018; Oliveira et al., 2019; Oliveira et al., 2023). New data obtained off Figueira da Foz could help in understanding how these mechanisms affect the composition and distribution of particles in the BNL. In the short temporal records of days 16 and 18, some variability on the recorded cyst assemblages in the BNL was observed with time (Figures 6A, B). This variability may be partially explained by cyst production in the upper water

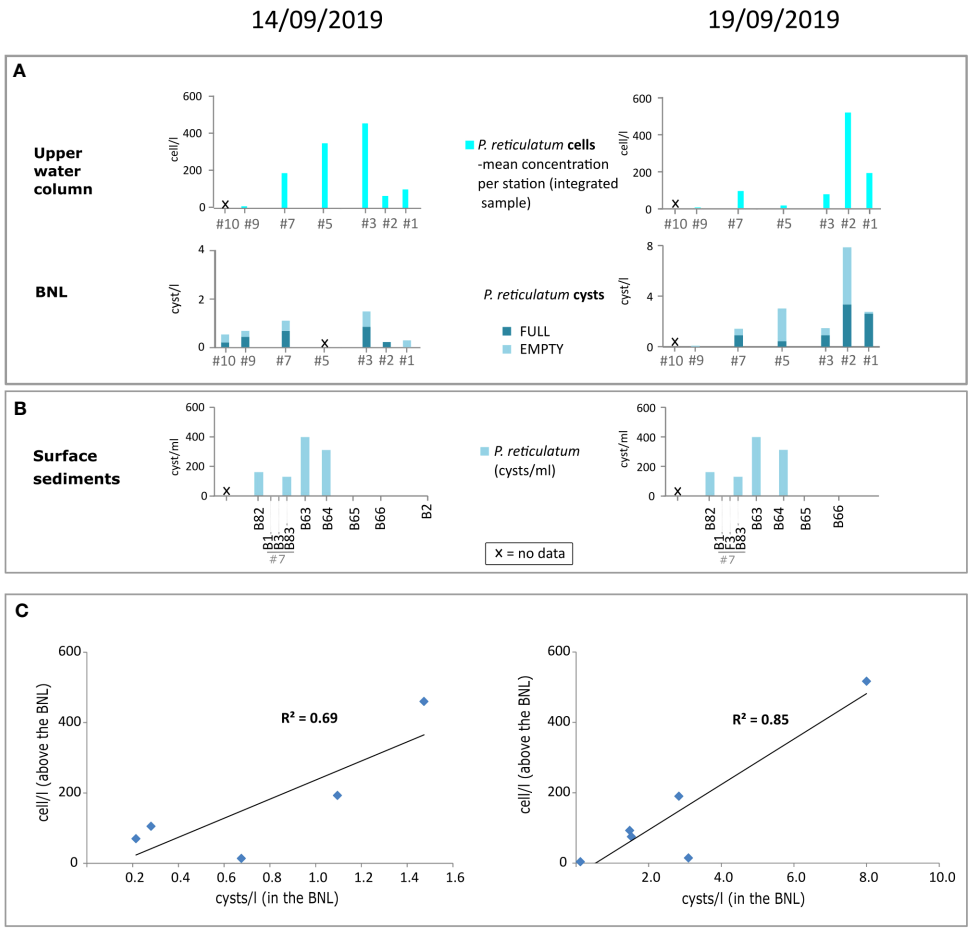

FIGURE 12
Distribution of cells of the toxic species *Protoceratium reticulatum* above the BNL (top bar diagram), and its cysts in the BNL **(A)** and the underlying sediments **(B)** along transects sampled on 14th (left) and 19th (right) of September 2019. Sampling stations along the horizontal axis were ordinated according to a land-sea gradient (right to left). Linear regressions of cell concentrations above the BNL vs. cyst concentrations in the BNL **(C)**, including the stations where both cyst and cell data were available. Plate 1 Microphotographs of selected dinoflagellate cysts from water samples (benthic nepheloid layer) collected off Figueira da Foz (NW Portugal): 1) empty *Diplopsalis*-type showing an elongated archeopyle, sample F2-12; 2) unidentified RBC with cell contents, sample F2-0; 3) full cyst of *Preperidinium meunieri (Dubridinium caperatum)*, sample F1-2 UP; 4) empty cyst of *Lejeunecysta sabrina*, sample F1-2 LOW; 5) full cyst of *Votadinium* cf. *rhomboideum*, sample S2; 6) full cyst of *Protoperidinium latidorsale* (*Votadinium calvum*), sample S2; 7) empty cyst of *Protoperidinium shangaiense* (*Trinovantedinium applanatum*); 8-9) full cyst of *Archaeperidinium constrictum*, sample F2-7; 10-11) empty cyst of *Protoperidinium monospinum*, sample F2-3; 12) full cyst of *P. conicum* (*Selenopemphix quanta*), sample S2; 13-14) unidentified empty SBC with short and solid spines, sample F2-7; 15-16) empty *Echinidinium transparantum/zonneveldiae*, sample F2-12; 17) full *Spiniferites* cf. *ramosus*, sample F2-9; 18) empty cyst of *Protoceratium reticulatum*, sample F2-7; 19) cyst of *Scripssiella* cf. *trochoidea*, sample F1-2; 20) full *Alex*-type, sample S2.

column, but other factors such as lateral transport could also contribute, bringing cysts from other areas to the sampling site. Regarding concentrations, notable changes were observed in a very short time, for example, the increase in SBC from 4 cysts/l to 49 cysts/l in just over 2 hours on day 16 (Figure 6A). It is possible that these differences in concentrations between these samples were due to the high variability of particle density within the BNL over time on the 16th September as shown in Figure 4. On the other hand, proportions of empty cysts varied between ~6% and 70% within all BNL samples (Figures 5, 6). They increased in samples collected on the 19th September in coastal stations T2-2 (~52%) and T2-3 (~67%) (Figure 5). In the fixed station #7, proportions of empty cysts increased in the lower layers of the BNL on the 16th of September (Figure 6A), and on the 18th over time, reaching the highest proportions (~52%) in the last sample (F2-12) collected at 13:16 h (Figure 6B).

The instrumented mooring deployed at station #7 and operated between 7th and 19th September, allowed high-temporal resolution records of temperature and acoustic backscattering intensity (used as a proxy for suspended particle concentration) in the first 100 m of the water column (Santos et al., 2022). These data indicated a relevant thermocline fluctuation around 12:45 h on the 18th September, representing the occurrence of an internal wave event (see Figure 2 in Santos et al., 2022). Despite the CTD record having a lower resolution than the ADCP, the CTD also recorded a slight but appreciable fluctuation in the thermocline at ~12:45 h of the same day (see Figure 4B, top diagram). According to the high-resolution ADCP data, the fluctuation recorded in the CTD probably does not reflect the maximum expression of the internal wave. The passage of the internal wave at 12:45 h coincided with an appreciable fluctuation in the BNL dinoflagellate cyst assemblage, i.e., a decrease in total cyst concentrations and an increase in the proportion of empty cysts (Figure 6B). Although the small number of samples does not allow us to confirm the relationship between these two events, this coincidence is very interesting from the point of view of the dynamics of the particles in the BNL. Further studies are needed to confirm this relationship. These should include recording cyst assemblages in the BNL during the passage of several internal waves and encompassing periods without internal wave activity. This would allow a quantitative approach and reaching more solid conclusions.

Our cyst record may be too short to establish a robust relationship between internal waves and cyst events; however, it already suggests that the study of dinoflagellate cyst assemblages may be very useful to understand the effects of internal waves on BNL dynamics. Moreover, new data lead us to raise the hypothesis that the passage of an internal wave could have effects on the distribution of cysts in the BNL, causing some dispersion of the BNL and local resuspension of sediments. The first fact would explain the observed decrease in cyst concentrations, and the second, the increase in empty cyst proportions (Figure 6B). Nevertheless, future work including longer time-series of cyst records in the BNL, encompassing more passages of internal waves of higher amplitude (and other physical fluctuations) at higher time resolution, would be needed to verify that internal waves do indeed influence cyst bed dynamics and contribute to the benthic-pelagic coupling of distinct life cycle stages in cyst-producing dinoflagellates.

In addition to sediment resuspension, cyst hatching in the water column could also explain part of the observed empty cysts in the BNL, such as those of *P. reticulatum* and SBC that increased over time (Figure 6). These taxa were proliferating in surficial waters and new cysts were being produced in the water column (Figure 7). Empty cysts of these types were very scarce in the sediments, thus the origin of these cysts in the BNL was likely not local sediment resuspension. Some observations on excystment dynamics performed on the field by using sediment traps have shown that some cysts, particularly heterotrophic species that included cysts of *Protoperidinium* spp. can hatch rapidly after being produced within the water column, before reaching deep waters (Price and Pospelova, 2011; Zonneveld et al., 2021; Zonneveld et al., 2022). From our observations, we cannot be sure how old the cysts found in the BNL were, but they were maintained in suspension in the BNL for at least 5-10 days (Figures 10, 11). Therefore, the hypothesis that some empty cysts found in the BNL came from hatching cannot be neglected.

However, it has been observed in the laboratory that most dinoflagellate cysts cannot hatch before finishing a mandatory dormancy period which varies from a few days to several months, depending on the species (Anderson, 1980; Blanco, 1990; Bravo and Anderson, 1994; Amorim et al., 2002; Figueroa and Bravo, 2005; Figueroa et al., 2008). The excystment experiments performed with cysts isolated from the BNL, showed that some cysts of *P. reticulatum* and SBC could germinate in only 3-7 days once they were transferred to higher temperature and light. This suggests cysts had already gone through the mandatory dormancy period before being isolated. The mandatory dormancy period could be much longer, if we consider that these cysts had been stored for several months before being isolated in the laboratory. Salgado et al. (2017) estimated a mandatory maturation period of ~4 months for the species *Protoceratium reticulatum*. According to this, the probability that empty cysts of *P. reticulatum* found in the BNL off Figueira da Foz came from the hatching of cysts recently formed in the water column is very low.

Another possible explanation for the rise in relative abundances of empty vs. full cysts in the BNL over time (Figures 5, 6) could be the high decay resistance nature of many cyst walls that would also promote the build-up of the empty cyst fraction. Finally, the contribution of allochthonous empty cysts that could have been resuspended in other places and laterally transported to the BNL of the studied transect must also be considered. In fact, as will be explained in the next section, our results supported that lateral transport is a relevant factor in explaining the distribution of cysts in the BNL.

5.2 Lateral transport affecting cyst distribution in the BNL

The highest cell concentrations of *Protoceratium reticulatum* were found on 14th September. As upwelling relaxed (19th September), the inshore side of the thermal front moved coastward (Figure 3), and the bloom of *P. reticulatum* approached the coast and became patchier (Figure 7) (Moita et al., 2022). As a

result of hydrographic changes and cell redistribution, the distribution of *P. reticulatum* cysts in the BNL also changed, with cyst concentrations notably increasing on 19th September at inshore stations (Figure 5B). Apparent spatial and temporal inconsistencies in the distributions of cysts and cells of *P. reticulatum* within the water column were observed. The highest cell concentrations (~2100 cells/l) were recorded on 14th September at mid-depth stations (#3 and #5) (Figure 7D), while cyst concentrations in the water column were very low at that moment (Figure 7C). In contrast, cysts notably increased on the 19th at inshore stations, both in the BNL (Figure 5B) and above (Figure 7C), when cell concentrations in the water column were diminishing (Figure 7D). This temporary mismatch between the cyst and cell distributions could be explained because once formed cysts need time to settle within the water column, as they act as passive particles (Dale, 1976; Anderson et al., 2005). Moreover, massive encystment can be linked to bloom termination (Heiskanen, 1993; Brosnahan et al., 2017), which would explain why cyst concentrations of *P. reticulatum* increased as vegetative cell abundances decreased over time in the water column (Figures 7C, D). This could also be a plausible explanation for the increase in the concentrations of other cyst types over time (see total cysts and SBC in Figures 7A, B). Furthermore, cyst distribution along the two studied transects could also be explained by the influence of lateral transport, as discussed in the following paragraphs.

Crosshore and alongshore movements of water masses are prominent features of coastal upwelling systems that control the transport, accumulation, and dispersion of planktonic communities (Escalera et al., 2010; Pitcher et al., 2010). During their downward trajectory to the seabed, particles are susceptible to lateral advection (e.g., Freudenthal et al., 2001; Nooteboom et al., 2019; Zonneveld et al., 2022). Lateral transport could partially explain the cyst distributions off Figueira da Foz. On 19th September, the highest concentrations of SBC and cysts of *P. reticulatum* in the BNL were found at more inshore sites (Figure 5B) than in the water column above, where peaks of these cysts occurred at more offshore sites (Figures 7B, C). Also, we observed a great increase in SBC concentrations at deeper waters and in more offshore stations over time (from 14th to 19th September, Figure 7B) that cannot be explained by vertical sinking alone. These apparent incongruences between the maxima of cyst abundances along the vertical of the water column could be due to lateral transport (Figure 12), which would bring cysts from other areas to the study site. Moreover, the fact that cyst concentrations in the BNL were generally much lower (10 times lower in the case of *P. reticulatum*) than in the upper water column suggested that cysts were being produced at the surface where the bloom developed and that extended latitudinally (Figure 2B). The cysts observed in the water column along the land-sea transect (Figure 7) could come from anywhere within the blooming area and been transported to the sampled sites by horizontal currents. Our results give strong supporting evidence that encystment of *P. reticulatum* and other cyst species was occurring in the water column and laterally advected.

Lateral transport could also explain the notable differences observed in the cyst distribution pattern between the water column (Figures 5, 7) and the underlying sediments (Figure 9) along the studied transects. In addition to the differences found in cyst taxa composition, reflected by clustering (Figure 10), cyst concentrations in sediments were generally higher at more offshore sites (>20 km from the coast, Figure 9B) than in the BNL, where the highest cyst concentrations occurred at more inshore stations (<20 km from the coast, Figure 5B). However, cyst records in surface sediments and water samples are, in principle, not comparable. Water samples reflect the cyst content at the time of sampling (on 14th or 19th September) and presumably do not integrate cyst production over long periods, while the surface sediment sample is the signature of cysts produced and accumulated over several years in the sedimentary system (Dale, 1976). According to estimated sedimentation rates the surface sediment samples off Figueira da Foz could represent between 2.5 and 20 years of cyst deposition (Jouanneau et al., 2002; García-Moreiras et al., 2021). In any case, the distribution of cells and cysts observed in this study (Figure 7) agreed with the typical spatial distribution of phytoplankton biomass along the inshore-offshore gradient off the study site during the upwelling season, which is the period that is assumed to have the greatest imprint in the sedimentary record (Abrantes and Moita, 1999). Chl-*a* and phytoplankton abundances are typically higher close to the coast, i.e.,<100 m depth (Abrantes and Moita, 1999; Oliveira et al., 2019; Nunes, 2021) (Figure 2A). The observed spatial mismatch between the maximum cell abundances in the water column (inshore) and the cyst accumulation in the sediments (offshore) (Figures 9B, 12A), supports the relevance of lateral transport on cyst distribution and accumulation patterns in the seabed. This emphasizes how cyst distribution in the sediments depends on both life-cycle and sedimentary dynamics (e.g., Anderson et al., 2005; Kirn et al., 2005; Bravo et al., 2010; Anderson et al., 2014; García-Moreiras et al., 2021).

The occurrence of lateral transport affecting cyst dynamics in the BNL off Figueira da Foz was supported by back-track particle modelling. According to Lagrangian experiments, alongshore transport (southwards inshore and northwards offshore) notably affected cyst distributions in deep waters. At inshore stations, where alongshore transport was intensified, cysts would have been transported longer distances before reaching the studied transect (Figures 11A, D). This is consistent with the presence of surface water currents running parallel to the coast at higher velocities than offshore, in response to the upwelling event that peaked on September 11th-12 th (Nunes, 2021). During the sampling campaign, as upwelling relaxed (Figures 2, 3) and alongshore transport decreased (Figure 11), cell abundances of *P. reticulatum* approached the coast (Figure 7D) and cyst concentrations in the BNL increased at inshore stations (Figure 5B). These results can be explained because wind relaxation reduces cell dispersion, promoting cell accumulation towards the coast (e.g., Fraga et al., 1988; Moita et al., 2003).

Global models had predicted an important influence of lateral transport on cyst distributions, and therefore on the local imprint left by planktonic communities in the sediments; this influence would be of greater magnitude in deep environments off the shelf (Nooteboom et al., 2019). Our study suggests that lateral transport in shelf environments may also be important and cannot be neglected when interpreting sedimentary records. The existence of

relevant lateral transport affecting cyst distribution in coastal environments implies that the sediment cyst records are a mixture of cysts produced *in-situ* and *ex-situ*. This is of relevance in paleoceanography for the reconstruction of the local environments from the sediment cyst records (e.g., Zonneveld and Brummer, 2000). Furthermore, another factor that could be affecting the sediment imprint of local dinoflagellate populations is selective degradation. In general, autotrophic cysts are more resistant to oxidation processes (e.g., Zonneveld and Brummer, 2000; Zonneveld et al., 2008), which could explain why heterotrophic cysts were generally less abundant in the sediments than in the water column (Figures 5, 9).

In contrast to the presence of significant alongshore transport, cyst distribution in the BNL during the studied period must have been affected by little vertical and across-shore transport (Figures 11B, C). The occurrence of a maximum divergence zone near the coast, at ~5-20 km offshore (Nunes, 2021) resulted in two water masses with different biological and environmental features: one colder coastal mass with higher primary productivity (Chl-*a* concentrations) and another situated more offshore (>100 m depth) with higher SST and lower primary productivity (Figures 2A, B). This probably conditioned the spatial distribution of biological communities, and therefore the cyst distribution in the BNL along the studied land-sea transect. Especially on 14th September, the cyst distribution in the BNL showed a marked land-sea gradient, with cyst concentrations and heterotrophic taxa markedly decreasing offshore (Figure 5). The divergence zone acts as a barrier for Ekman transport preventing the transport of particles offshore (Estrade et al., 2008), explaining the higher cyst and cell concentrations recorded inshore in the water column (Figures 5B, 7), and the great differences found in cyst assemblages between inshore and offshore sites (Figures 5A, 10). This is consistent with the little across-shore transport inferred by back-track particle modelling off Figueira da Foz (Figure 11B). Upwelling filaments can also promote offshore transport of particles (Rossi et al., 2013; Zonneveld et al., 2018; Villacieros-Robineau et al., 2019); however, no pronounced filaments affecting the studied transect were detected before 14th September, according to satellite-derived Chl-*a* data (Figure 2B).

In summary, new multi-proxy data supported that alongshore transport was the main physical forcing affecting cyst dynamics off Figueira da Foz during the survey in September 2019, and corroborated the strong influence of upwelling-downwelling pulses and local hydrodynamics on biota distribution, in agreement with previous studies (Bravo et al., 2010; Escalera et al., 2010; Bringué et al., 2019; Oliveira et al., 2019; Zonneveld et al., 2022).

5.3 The BNL as a reservoir of viable cysts: implications for understanding bloom dynamics

This study revealed the occurrence of many full cysts in the BNL along the land-sea transect studied off Figueira da Foz (Figures 5B, 7). Eight cyst types were successfully germinated under laboratory conditions (Table 3), confirming their viability. Although only 27% of all isolated cysts germinated, these low germination rates can be —at least partially— explained because the germination experiments had to be suspended as a consequence of the Covid-19 lockdown starting in March 2020. The last check on germination was done on 13th March 2020 when many cysts had only been incubated for a few days. Furthermore, long storage periods of >1 month may in some cases have affected the germination success (Blanco, 1990; Amorim et al., 2001). In this study, cysts were stored during 4-5.5 months between sampling (14th-19th of September 2019) and isolation (20th of January-6th of March). In any case, our observations confirmed that a significant number of the isolated full cysts from the BNL were viable, that is, they had the potential to germinate and initiate a planktonic population.

Cyst germination is controlled by internal mechanisms, but can also be triggered by external factors such as exposure to light, turbulence and temperature change (Dale, 1983; Pfiester and Anderson, 1987; Matsuoka and Fukuyo, 2000; Fischer et al., 2018). Cyst germination in the sediments is prevented by darkness, lower oxygen availability and low temperatures (Anderson and Morel, 1979; Anderson et al., 1987; Bravo and Anderson, 1994; Rengefors et al., 2004; Anderson et al., 2005). Benthic cysts can be resuspended and transported by physical processes —such as currents, upwelling events or internal waves— to the upper water column (Nehring, 1996; Giannakourou et al., 2005) where they can find the environmental conditions they need to germinate. Suspended cysts in the BNL are exposed to oxygen and are closer to the euphotic layer, so they do not have to escape the sediment matrix to find favorable conditions for germination. This can lead to higher germination rates and germling survival than in the bottom sediments. For this reason, it has been hypothesized that cysts in the BNL could have an important role in the maintenance of planktonic populations, providing the necessary inoculum to start planktonic blooms (Kirn et al., 2005; Pilskaln et al., 2014a; Pilskaln et al., 2014b).

The absence of significant beds of viable cysts in the sediments off Figueira da Foz (García-Moreiras et al., 2021), has led to the proposal of alternative mechanisms for seeding of local planktonic blooms, such as the advection of allochthonous populations, as it has been proposed for certain species. This is the case of non-cyst-producing species (e.g., Escalera et al., 2010) and when cyst beds are not found close to where the blooms are produced (Smayda, 2002; Smayda and Reynolds, 2003; Figueroa et al., 2008). Another option would be for the cyst bed not to be found in the sediments but rather suspended in the BNL. In this sense, this study documents the presence of cysts with cell contents in the BNL and that a significant number was viable for germination. Moreover, we provided evidence supporting that the full cysts recently formed in the photic zone could be laterally advected within the studied region. In the most inshore sites, the source of those cysts during the studied period was probably from sites further north to the study area (Figure 11).

There is little data on cyst residence times in the BNL, which can be highly variable between different regions (Pilskaln et al., 2014a). In Figueira da Foz, according to the Langrangian particle transport model (Figure 11), some cysts remained in suspension in the BNL for at least 10 days. The BNL may transport cysts from where they are produced to other areas where, if the right environmental conditions are met, they may originate new

planktonic populations. Therefore, our observations are compatible with the BNL acting as a reservoir of viable cysts that have the potential to seed new planktonic populations.

In any case, the seeding strategy and the type of propagule (vegetative cells and resting cysts) on which phytoplankton communities rely can vary throughout the year, and may depend on the intensity of the upwelling/relaxation event and the dinoflagellate species (e.g., Bravo et al., 2010; Smayda and Trainer, 2010; Diaz et al., 2014). Further studies involving longer time-series records of the cyst and vegetative cell assemblages (benthic and planktonic), possibly combining sediment trap data from different water depths, would help in evaluating the seeding potential of the BNL for the initiation of dinoflagellate blooms on the Atlantic Iberian margin and other Eastern Boundary Upwelling Systems.

Results presented herein on physical and cyst data obtained off Figueira da Foz bring new insights into the effect of internal waves on BNL particle distribution with possible influence on the dynamics of cyst producing dinoflagellates, many of which may be nuisance. The West Iberian coast is characterized by seasonal upwelling and high internal wave activity and these results may be of relevance in comparable regions of the world, where the BNL is an ubiquitous feature (Oliveira et al., 2002; Oliveira et al., 2007; Villacieros-Robineau et al., 2019; Tian et al., 2022; Oliveira et al., 2023; and references therein). Internal waves are common in shelf environments and their propagation is favored by stratification of the water column (e.g., Oliveira et al., 2002; Vitorino et al., 2002; Jackson, 2007; Jackson et al., 2012; Lamb, 2014). Stratification is also an important environmental factor for the growth of many dinoflagellates during summer and fall, particularly in the case of the toxic autotrophic dinoflagellate species, such as *Protoceratium reticulatum*, *Gymnodinium catenatum* and *Lingulodinium polyedra*. These and other cyst-forming species usually proliferate in coastal environments influenced by upwelling following the nutrient enrichment events when waters are becoming stratified (Smayda and Reynolds, 2001; Amorim et al., 2001; Moita et al., 2003; Smayda and Reynolds, 2003; Moita et al., 2022; Mertens et al., 2023; etc.).

The highest rates of encystment and cyst flux to the sediments occurs during and after bloom events (Amorim et al., 2001; Anderson et al., 2005; Peña-Manjarrez et al., 2009; Brosnahan et al., 2017; Mertens et al., 2023). Therefore, propagation of internal waves in coastal environments may coincide with increased cyst productivity, as both events are favored by stratification conditions. The evidence presented herewith suggesting internal waves could affect the distribution of cysts in the BNL through local resuspension, highlights their potential influence on the transport and dynamics of cyst-forming species in other coastal regions in the world.

6 Conclusions

Combined *in-situ* observations (physical data and dinoflagellate cyst records) and back-track particle modelling, allowed studying the main biological and physical factors affecting spatial and temporal dinoflagellate cyst distributions in the bottom nepheloid layer (BNL) along a land-sea transect off Figueira da Foz (Atlantic Iberian margin). A well-developed BNL was present during the survey (14^{th}-19^{th} of September 2019), which covered a change from active to relaxed upwelling conditions. Most cyst assemblages in the BNL were dominated by heterotrophic taxa, among which the most abundant type was small spiny brown cysts (SBC). SBC and cysts of the autotrophic yessotoxin producer *Protoceratium reticulatum* notably increased during the survey, in the BNL and in the water column above. Several lines of evidence supported that the main source of dinoflagellate cysts in the BNL was recent encystment in the water column during most of the survey period: 1) high proportions of full cysts, 2) the statistical similarities between most of the BNL cyst records and the cyst rain recorded by a sediment trap, and 3) the spatial coincidences in the distribution of cysts and vegetative cells of *P. reticulatum*. Moreover, excystment experiments showed that a significant portion was viable; therefore, the presence of a reservoir of viable cysts in the BNL with the potential to seed new planktonic blooms cannot be discarded. According to the Langrangian particle transport model some cysts could remain in suspension in the BNL for at least 10 days. Clustering revealed that most of the BNL cyst records were different from the sediment cyst assemblages, thus supporting that they were not significantly affected by local sediment resuspension. Exceptions were samples collected on 14^{th} September in the deepest (>100 m depth) and shallowest (<30 m) stations, which would have been influenced by local sediment cyst resuspension.

Finally, back-track particle modelling allowed identifying alongshore transport as the main physical mechanism controlling cyst dynamics in the BNL during most part of the survey period. This alongshore (southwards) transport was more intense in coastal stations (<100 m depth); in contrast, in offshore sites (>100 m depth) alongshore transport was less intense and cysts were advected northwards. In consequence, the sediment cyst signal is a mixture of locally and regionally produced cysts, which may have implications in paleoceanographic reconstructions from dinoflagellate cyst sediment records. New multidisciplinary data evidenced that full cysts recently formed in the photic zone can be laterally advected through the BNL, and that the relevance of physical processes (i.e., lateral transport and resuspension) affecting cyst distribution in the BNL changed spatially and temporally, being closely linked to coastal upwelling dynamics.

Data availability statement

The datasets presented in this study can be found in online repositories. The names of the repository/repositories and accession number(s) can be found below: https://doi.org/10.1594/PANGAEA.963768, https://doi.org/10.1594/PANGAEA.963833.

Author contributions

IG-M: Formal Analysis, Investigation, Methodology, Visualization, Writing – original draft. MH: Investigation,

Methodology, Writing – review and editing. KZ: Investigation, Writing – review and editing, Methodology. JD: Conceptualization, Formal Analysis, Investigation, Methodology, Writing – review and editing, Resources. RN: Formal Analysis, Investigation, Methodology, Visualization, Writing – review and editing. AS: Investigation, Methodology, Writing – review and editing. AO: Conceptualization, Formal Analysis, Investigation, Methodology, Visualization, Writing – review and editing. TM: Investigation, Methodology, Writing – review and editing, Conceptualization, Formal Analysis. PO: Conceptualization, Formal Analysis, Funding acquisition, Investigation, Methodology, Project administration, Resources, Supervision, Validation, Writing – review and editing. JM: Formal Analysis, Investigation, Methodology, Visualization, Writing – review and editing. AA: Conceptualization, Formal Analysis, Funding acquisition, Investigation, Methodology, Project administration, Resources, Supervision, Validation, Writing – review and editing.

Funding

The author(s) declare financial support was received for the research, authorship, and/or publication of this article. This work is a contribution to HABWAVE project LISBOA-01-0145-FEDER-031265, co-funded by EU ERDF funds, within the PT2020 Partnership Agreement and Compete 2020, and national funds through Fundação para a Ciência e Tecnologia, I.P.(FCT, I.P.) also to AQUIMAR project MAR2020; MAR-02.01.01-FEAMP-017. This study had the support of FCT through the strategic projects UIDB/04292/2020 and UIDP/04292/2020 awarded to MARE and through project LA/P/0069/2020 granted to the Associate Laboratory ARNET, the strategic project UIDB/04326/2020 awarded to CCMAR. Thanks are also due for the financial support to CESAM by FCT/MCTES (UIDP/50017/2020+UIDB/50017/2020 +LA/P/0094/2020), Partnership Agreement and Compete 2020. IG-M was supported by a postdoctoral fellowship from Xunta de Galicia, Spain (ref. ED481B-2019-074, 2019). JM gratefully acknowledges the Fundação para a Ciência e Tecnologia and its support via strategic funding UIDB/04423/2020 and UIDP/04423/2020, and project MIWAVES (PTDC/2022.01215.PTDC).

Acknowledgments

We thank all the researchers, students and the crew of "N. O. Auriga", who were most helpful in ensuring the success of the cruise. Special thanks to Dr. Donald Anderson (Woods Hole Oceanographic Institution, USA) for the scientific supervision of the project, constant availability and constructive discussions.

Conflict of interest

The authors declare that the research was conducted in the absence of any commercial or financial relationships that could be construed as a potential conflict of interest.

The author(s) declared that they were an editorial board member of Frontiers, at the time of submission. This had no impact on the peer review process and the final decision.

Publisher's note

Supplementary material

The Supplementary Material for this article can be found online at: https://www.frontiersin.org/articles/10.3389/fmars.2023.1270343/full#supplementary-material

References

Abrantes, F., and Moita, M. T. (1999). Water column and recent sediment data on diatoms and coccolithophorids, off Portugal, confirm sediment record of upwelling events. *Oceanol. Acta* 22 (3), 319–336. doi: 10.1016/S0399-1784(99)80055-3

Álvarez-Salgado, X. A., Labarta, U., Fernández-Reiriz, M. J., Figueiras, F. G., Rosón, G., Piedracoba, S., et al. (2008). Renewal time and the impact of harmful algal blooms on the extensive mussel raft culture of the Iberian coastal upwelling system (SW Europe). *Harmful Algae* 7 (6), 849–855. doi: 10.1016/j.hal.2008.04.007

Amorim, A. (2001). Dinoflagellate cyst distribution along the coast of Portugal. PhD thesis (Lisbon: University of Lisbon, Portugal). 178 pp.

Amorim, A., Dale, B., Godinho, R., and Brotas, V. (2002). *Gymnodinium catenatum*-like cysts (Dinophyceae) in recent sediments from the coast of Portugal. *Phycologia* 40 (6), 572–582. doi: 10.2216/i0031-8884-40-6-572.1

Amorim, A., Moita, M. T., and Oliveira, P. (2004). "Dinoflagellate blooms related to coastal upwelling plumes off Portugal," in *Harmful Algae 2002*. Eds. K. A. Steidinger, J. H. Landsberg, C. R. Tomas and G. A. Vargo (St. Petersburg, Florida: Florida Fish and Wildlife Conservation Commission, Florida Institute of Oceanography, and Intergovernmental Oceanographic Commission of UNESCO), 89–91.

Amorim, A., Palma, A. S., Sampayo, M. A., and Moita, M. T. (2001). "On a *Lingulodinium polyedrum* bloom in Setúbal bay, Portugal," in *Proceedings of the 9th International Conference on Harmful Algal Blooms*, Hobart, Australia, 7-11 February 2000. Eds. G. M. Hallegraeff, S. I. Blackburn, C. J. Bolch and R. J. Lewis (Intergovernmental Oceanographic Commission of UNESCO), 133–136.

Anderson, D. M. (1980). Effects of temperature conditioning on development and germination of *Gonyaulax tamarensis* (Dinophyceae) hypnozygotes. *J. Phycol.* 16, 166–172. doi: 10.1111/j.1529-8817.1980.tb03013.x

Anderson, D. M. (1984). "Shellfish toxicity and dormant cysts in toxic dinoflagellate blooms," in *Seafood Toxins*, vol. 262 . Ed. E. P. Ragelis (Wash. D.C: Amer. Chem. Soc), 125–138.

Anderson, D. M., Lively, J. J., Reardon, E. M., and Price, C. A. (1985). Sinking characteristics of dinoflagellate cysts 1. *Limnol. Oceanogr.* 30 (5), 1000–1009.

Anderson, D. M. (2014). "HABs in a changing world: a perspective on harmful algal blooms, their impacts, and research and management in a dynamic era of climatic and environmental change," in *Harmful Algae: Proceedings of the 15th International Conference on Harmful Algae* (Busan, Korea: International Society for the Study of Harmful Algae), 3–17.

Anderson, D. M., Jacobson, D. M., Bravo, I., and Wrenn, J. H. (1988). The unique micro reticulate cyst of the naked dinoflagellate *Gymnodinium catenatum*. *J. Phycol.* 24, 255–262. doi: 10.1111/j.1529-8817.1988.tb00085.x

Anderson, D. M., Keafer, B. A., Kleindinst, J. L., McGillicuddy, J. D. J., Martin, J. L., Norton, K., et al. (2014). *Alexandrium fundyense* cysts in the Gulf of Maine: long-term time series of abundance and distribution, and linkages to past and future blooms. *Deep Sea Res. Part II: Topical Stud. Oceanogr.* (Busan, Korea: International Society for the Study of Harmful Algae) 103, 6–26. doi: 10.1016/j.dsr2.2013.10.002

Anderson, D. M., and Morel, F. (1979). The seeding of two red tide blooms by the germination of benthic *Gonyaulax tamarensis* hypnozygotes. *Estuar. Coast. Mar. Sci.* 8, 279–293. doi: 10.1016/0302-3524(79)90098-7

Anderson, D. M., Stock, C. A., Keafer, B. A., Nelson, A. B., Thompson, B., McGillicuddy, D. J. Jr., et al. (2005). *Alexandrium fundyense* cyst dynamics in the Gulf of Maine. *Deep Sea Res. Part II: Topical Stud. Oceanogr.* 52 (19–21), 2522–2542. doi: 10.1016/j.dsr2.2005.06.014

Anderson, D. M., Taylor, C. D., and Armbrust, E. V. (1987). The effects of darkness and anaerobiosis on dinoflagellate cyst germination. *Limnol. Oceanogr.* 32 (2), 340–351. doi: 10.4319/lo.1987.32.2.0340

Berdalet, E., Montresor, M., Reguera, B., Roy, S., Yamazaki, H., Cembella, A., et al. (2017). Harmful algal blooms in fjords, coastal embayments, and stratified systems: Recent progress and future research. *Oceanography* 30 (1), 46–57. doi: 10.5670/oceanog.2017.109

Blanco, J. (1990). Cyst germination of two dinoflagellate species from Galicia (NW Spain). *Sci. Mar.* 54 (3), 287–291.

Blanco, J. (1995a). Cyst production in four species of neritic dinoflagellates. *J. Plankton Res.* 17 (1), 165–182. doi: 10.1093/plankt/17.1.165

Blanco, J. (1995b). The distribution of dinoflagellate cysts along the Galician (NW Spain) coast. *J. Plankton Res.* 17 (2), 283–302. doi: 10.1093/plankt/17.2.283

Bolch, C. J. S. (1997). The use of sodium polytungstate for the separation and concentration of living dinoflagellate cysts from marine sediments. *Phycologia* 36, 472–478. doi: 10.2216/i0031-8884-36-6-472.1

Bolch, C. J., Blackburn, S. I., Cannon, J. A., and Hallegraeff, G. M. (1991). The resting cyst of the red-tide dinoflagellate *Alexandrium minutum* (Dinophyceae). *Phycologia* 30 (2), 215–219. doi: 10.2216/i0031-8884-30-2-215.1

Botelho, M. J., Vale, C., and Ferreira, J. G. (2019). Seasonal and multi-annual trends of bivalve toxicity by PSTs in Portuguese marine waters. *Sci. Total Environ.* 664, 1095–1106. doi: 10.1016/j.scitotenv.2019.01.314

Bravo, I., and Anderson, D. M. (1994). The effects of temperature, growth medium and darkness on excystment and growth of the toxic dinoflagellate *Gymnodinium catenatum* from northwest Spain. *J. Plankton Res.* 16 (5), 513–525. doi: 10.1093/plankt/16.5.513

Bravo, I., and Figueroa, R. I. (2014). Towards an ecological understanding of dinoflagellate cyst functions. *Microorganisms* 2, 11–32. doi: 10.3390/microorganisms2010011

Bravo, I., Fraga, S., Figueroa, R. I., Pazos, Y., Massanet, A., and Ramilo, I. (2010). Bloom dynamics and life cycle strategies of two toxic dinoflagellates in a coastal upwelling system (NW Iberian Peninsula). *Deep Sea Res. Part II: Topical Stud. Oceanogr.* 57, 222–234. doi: 10.1016/j.dsr2.2009.09.004

Bravo, I., Garcés, E., Diogène, J., Fraga, S., Sampedro, N., and Figueroa, R. I. (2006). Resting cysts of the toxigenic dinoflagellate genus *Alexandrium* in recent sediments from the Western Mediterranean coast, including the first description of cysts of *A. kutnerae* and *A. Peruvianum*. *Eur. J. Phycol.* 41 (3), 293–302. doi: 10.1080/09670260600810360

Bringué, M., Pospelova, V., Tappa, E. J., and Thunell, R. C. (2019). Dinoflagellate cyst production in the Cariaco Basin: a 12.5 year-long sediment trap study. *Prog. Oceanogr.* 171, 175–211. doi: 10.1016/j.pocean.2018.12.007

Brosnahan, M. L., Fischer, A. D., Lopez, C. B., Moore, S. K., and Anderson, D. M. (2020). Cyst-forming dinoflagellates in a warming climate. *Harmful Algae* 91, 101728. doi: 10.1016/j.hal.2019.101728

Brosnahan, M. L., Ralston, D. K., Fischer, A. D., Solow, A. R., and Anderson, D. M. (2017). Bloom termination of the toxic dinoflagellate *Alexandrium catenella*: vertical migration behaviour, sediment infiltration, and benthic cyst yield. *Limnol. Oceanogr.* 62 (6), 2829–2849. doi: 10.1002/lno.10664

Carr, S., Capet, X., McWilliams, J., Pennington, J., and Chavez, F. (2008). The influence of diel vertical migration on zooplankton transport and recruitment in an upwelling region: estimates from a coupled behavioral-physical model. *Fish. Oceanogr.* 17, 1–15. doi: 10.1111/j.1365-2419.2007.00447.x

Cordeiro, N. G. F., Nolasco, R., Barton, E. D., and Dubert, J. (2021). Fixed-point time series, repeat survey and high-resolution modelling reveal event scale responses of the Northwestern Iberian upwelling. *Prog. Oceanogr.* 190, 102480. doi: 10.1016/j.pocean.2020.102480

Crespo, B. G., Figueiras, F. G., Porras, P., and Teixeira, I. G. (2006). Downwelling and dominance of autochthonous dinoflagellates in the NW Iberian margin: the example of the Ría de Vigo. *Harmful Algae* 5 (6), 770–781. doi: 10.1016/j.hal.2006.03.006

Cunha, P. P., and Dinis, J. (2002). "Sedimentary dynamics of the Mondego estuary," in *Aquatic Ecology of the Mondego River Basin. Global Importance of Local Experience*. Eds. M. A. Pardal, M. A. S. Graça and J. C. Marques Coimbra (Portugal: Imprensa da Universidade de Coimbra), 43–63. doi: 10.14195/978-989-26-0336-0_4

Dale, B. (1976). Cyst formation, sedimentation, and preservation: factors affecting dinoflagellate assemblages in recent sediments from Trondheimsfjord, Norway. *Rev. Palaeobot. Palynol.* 22, 39–60. doi: 10.1016/0034-6667(76)90010-5

Dale, B. (1983). "Dinoflagellate resting cysts:" benthic plankton"," in *Survival strategies of the algae*. Ed. A. Fryxell (USA: Cambridge University Press), 69–136.

Dale, B. (1996). "Dinoflagellate cyst ecology: modelling and geological applications." in *Palynology: principles and applications*. Eds. J. Jansonius and D. G. McGregor (Dallas, USA: American Association of Stratigraphic Palynologists (AASP) Foundation). vol 3, 1249–1275.

Diaz, P. A., Molinet, C., Seguel, M., Diaz, M., Labra, G., and Figueroa, R. I. (2014). Coupling planktonic and benthic shifts during a bloom of *Alexandrium catenella* in southern Chile: Implications for bloom dynamics and recurrence. *Harmful algae* 40, 9–22. doi: 10.1016/j.hal.2014.10.001

Escalera, L., Reguera, B., Moita, T., Pazos, Y., Cerejo, M., Cabanas, J. M., et al. (2010). Bloom dynamics of *Dinophysis acuta* in an upwelling system: in *situ* growth versus transport. *Harmful Algae* 9, 312–322. doi: 10.1016/j.hal.2009.12.002

Estrade, P., Marchesiello, P., De Verdière, A. C., and Roy, C. (2008). Cross-shelf structure of coastal upwelling: A two-dimensional extension of Ekman's theory and a mechanism for inner shelf upwelling shut down. *J. Mar. Res.* 66 (5), 589–616. doi: 10.1357/002224008787536790

Ferreira, A., Brotas, V., Palma, C., Borges, C., and Brito, A. C. (2021). Assessing phytoplankton bloom phenology in upwelling-influenced regions using ocean color remote sensing. *Remote Sens.* 13, 675. doi: 10.3390/rs13040675

Ferreira Cordeiro, N. G., Dubert, J., Nolasco, R., and Desmond Barton, D. E. (2018). Transient response of the Northwestern Iberian upwelling regime. *PloS One* 13 (6), e0199806. doi: 10.1371/journal.pone.0197627

Figueiras, F. G., Labarta, U., and Reiriz, M. F. (2002). Coastal upwelling, primary production and mussel growth in the Rías Baixas of Galicia. *Hydrobiologia* 484, 121–131. doi: 10.1023/A:1021309222459

Figueiras, F. G., and Pazos, Y. (1991). Microplankton assemblages in three Rias Baixas (Vigo, Arosa and Muros, Spain) with a subsurface chlorophyll maximum: their relationships to hydrography. *Marine. Ecol. Prog. Ser.* 76, 219–233. doi: 10.3354/meps076219

Figueroa, R. I., and Bravo, I. (2005). Sexual reproduction and two different encystment strategies of *Lingulodinium polyedrum* (dinophyceae) in culture. *J. Phycol.* 41 (2), 370–379. doi: 10.1111/j.1529-8817.2005.04150.x

Figueroa, R. I., Bravo, I., Ramilo, I., Pazos, Y., and Moroño, A. (2008). New life-cycle stages of *Gymnodinium catenatum* (Dinophyceae): laboratory and field observations. *Aquat. Microbial. Ecol.* 52 (1), 13–23. doi: 10.3354/ame01206

Fischer, A. D., Brosnahan, M. L., and Anderson, D. M. (2018). Quantitative response of *Alexandrium catenella* cyst dormancy to cold exposure. *Protist* 169 (5), 645–661. doi: 10.1016/j.protis.2018.06.001

Fiúza, A. F. G., Macedo, M. E., and Guerreiro, M. R. (1982). Climatological space and time variation of the Portuguese coastal upwelling. *Oceanol. Acta* 5, 31–50.

Flynn, K. J., Mitra, A., Anestis, K., Anschütz, A. A., Calbet, A., Duarte Ferreira, G., et al. (2019). Mixotrophic protists and a new paradigm for marine ecology: where does plankton research go now? *J. Plankton Res.* 41 (4), 375–391. doi: 10.1093/plankt/fbz026

Fraga, S., Anderson, D. M., Bravo, I., Reguera, B., Steidinger, K. A., and Yentsch, C. M. (1988). Influence of upwelling relaxation on dinoflagellates and shellfish toxicity in Ria de Vigo, Spain. *Estuar. Coast. Shelf Sci.* 27 (4), 349–361. doi: 10.1016/0272-7714(88)90093-5

Freudenthal, T., Neuer, S., Meggers, H., Davenport, R., and Wefer, G. (2001). Influence of lateral particle advection and organic matter degradation on sediment accumulation and stable nitrogen isotope ratios along a productivity gradient in the Canary Islands region. *Mar. Geol.* 177, 93–109. doi: 10.1016/S0025-3227(01)00126-8

García-Moreiras, I., Oliveira, A., Santos, A. I., Oliveira, P. B., and Amorim, A. (2021). Environmental factors affecting spatial dinoflagellate cyst distribution in surface sediments off aveiro-figueira da foz (atlantic iberian margin). *Front. Mar. Sci.* 8. doi: 10.3389/fmars.2021.699483

Gardner, W. D., Richardson, M. J., and Mishonov, A. V. (2018). Global assessment of benthic nepheloid layers and linkage with upper ocean dynamics. *Earth Planet. Sci. Lett.* 482, 126–134. doi: 10.1016/j.epsl.2017.11.008

Giannakourou, A., Orlova, T. Y., Assimakopoulou, G., and Pagou, K. (2005). Dinoflagellate cysts in recent marine sediments from Thermaikos Gulf, Greece: effects of resuspension events on vertical cyst distribution. *Continent. Shelf Res.* 25 (19–20), 2585–2596. doi: 10.1016/j.csr.2005.08.003

Gu, H., Kai, H., Bernd, K., Gwenael, B., Vera, P., Zhen, L., et al. (2021). Cyst-theca relationships of Spiniferites bentorii, S. hyperacanthus, S. ramosus, S. scabratus and molecular phylogenetics of Spiniferites and *Tectatodinium* (Gonyaulacales, Dinophyceae). *Phycologia* 60 (4), 332-353. doi: 10.1080/00318884.2021.1930796

Gurdebeke, P., Mertens, K. N., Pospelova, V., Matsuoka, K., Li, Z., Gribble, K. E., et al. (2019). Taxonomic revision, phylogeny, and cyst wall composition of the dinoflagellate cyst genus *Votadinium* Reid (Dinophyceae, Peridiniales, Protoperidiniaceae). *Palynology* 44 (2), 310-335. doi: 10.1080/01916122.2019.1580627

Hasle, G. R. (1978). "Phytoplankton Manual. VI," in *Monographs on Oceanic Methodology*. Ed. A. Sournia (Paris: UNESCO), 191–196.

Head, M. J. (1996). "Modern dinoflagellate cysts and their biological affinities," in *Palynology: Principles and Applications*, vol. 3 . Eds. J. Jansonius and D. C. McGregor (Dallas: AASP Foundation), 1197–1248.

Heiskanen, A. S. (1993). Mass encystment and sinking of dinoflagellates during a spring bloom. *Mar. Biol.* 116, 161–167. doi: 10.1007/BF00350743

Jackson, C. (2007). Internal wave detection using the moderate resolution imaging spectroradiometer (MODIS). *J. Geophys. Res.: Oceans* 112 (C11). doi: 10.1029/2007JC004220

Jackson, C. R., Da Silva, J. C., and Jeans, G. (2012). The generation of nonlinear internal waves. *Oceanography* 25 (2), 108–123. doi: 10.5670/oceanog.2012.46

Jeong, H. J., Du Yoo, Y., Park, J. Y., Song, J. Y., Kim, S. T., Lee, S. H., et al. (2005). Feeding by phototrophic red-tide dinoflagellates: five species newly revealed and six species previously known to be mixotrophic. *Aquat. Microbial. Ecol.* 40 (2), 133–150. doi: 10.3354/ame040133

Jouanneau, J. M., Weber, O., Drago, T., Rodrigues, A., Oliveira, A., Dias, J. M. A., et al. (2002). Recent sedimentation and sedimentary budgets on the western Iberian shelf. *Prog. Oceanogr.* 52 (2–4), 261–275. doi: 10.1016/S0079-6611(02)00010-1

Joyce, L. B., and Pitcher, G. C. (2004). Encystment of *Zygabikodinium lenticulatum* (Dinophyceae) during a summer bloom of dinoflagellates in the southern Benguela upwelling system. *Estuarine Coast. Shelf Sci.* 59 (1), 1–11. doi: 10.1016/j.ecss.2003.07.001

Karakaş, G., Nowald, N., Schäfer-Neth, C., Iversen, M., Barkmann, W., Fischer, G., et al. (2009). Impact of particle aggregation on vertical fluxes of organic matter. *Prog. Oceanogr.* 83 (1-4), 331–341.

Kirn, S. L., Townsend, D. W., and Pettigrew, N. R. (2005). Suspended Alexandrium spp. hypnozygote cysts in the Gulf of Maine. *Deep Sea Res. Part II: Topical Stud. Oceanogr.* 52 (19–21), 2543–2559. doi: 10.1016/j.dsr2.2005.06.009

Kremp, A. (2001). "Effects of cyst resuspension on germination and seeding of two bloom-forming dinoflagellates in the Baltic Sea," in *Marine Ecology Progress Series*, vol. 216. , 57–66. Available at: https://www.jstor.org/stable/24864738.

Lamb, K. G. (2014). Internal wave breaking and dissipation mechanisms on the continental slope/shelf. *Annu. Rev. Fluid Mech.* 46, 231–254. doi: 10.1146/annurev-fluid-011212-140701

Lundholm, N., Ribeiro, S., Andersen, T. J., Koch, T., Godhe, A., Ekelund, F., et al. (2011). Buried alive–germination of up to a century-old marine protist resting stages. *Phycologia* 50, 629–640. doi: 10.2216/11-16.1

Magalhaes, J. M., da Silva, J. C. B., Nolasco, R., Dubert, J., and Oliveira, P. B. (2022). "On the variability of internal waves on the western Portuguese shelf," in *7as Jornadas de Engenharia Hidrográfica/2as Jornadas Luso-Espanholas de Hidrografia*, (Lisbon Portugal), pp. 101-104. Available at: https://jornadas.hidrografico.pt/recursos/files/documentos/2022/7JEH-Livro_Atas.pdf

Magalhaes, J. M., Pires, A. C., da Silva, J. C. B., Buijsman, M. C., and Oliveira., P. B. (2021). Using SAR imagery to survey internal solitary wave interactions: A case study off the Western Iberian shelf. *Continent. Shelf Res.* 220, 104396. doi: 10.1016/j.csr.2021.104396

Matsuoka, K., and Fukuyo, Y. (2000). *Technical guide for modern dinoflagellate cyst study* Vol. 47 (Tokyo, Japan: Japan Society for the Promotion of Science). WESTPAC-HAB/WESTPAC/IOC 2000.

Mendes, R., Sousa, M. C., deCastro, M., Gómez-Gesteira, M., and Dias, J. M. (2016). New insights into the Western Iberian Buoyant Plume: Interaction between the Douro and Minho River plumes under winter conditions. *Prog. Oceanogr.* 141, 30–43. doi: 10.1016/j.pocean.2015.11.006

Mertens, K. N., Gu, H., Gurdebeke, P. R., Takano, Y., Clarke, D., Aydin, H., et al. (2020). A review of rare, poorly known, and morphologically problematic extant marine organic-walled dinoflagellate cyst taxa of the orders Gymnodiniales and Peridiniales from the Northern Hemisphere. *Mar. Micropaleontol.* 159, 101773. doi: 10.1016/j.marmicro.2019.101773

Mertens, K. N., Retho, M., Manach, S., Zoffoli, M. L., Doner, A., Schapira, M., et al. (2023). An unprecedented bloom of *Lingulodinium polyedra* on the French Atlantic coast during summer 2021. *Harmful Algae* 125, 102426. doi: 10.1016/j.hal.2023.102426

Moita, M. T. (1993). "Development of toxic dinoflagellates in relation to upwelling patterns off Portugal," in *Toxic phytoplankton blooms in the sea*. Eds. T. J. Smayda and Y. Shimizu (New York: Elsevier), 299–304.

Moita, M. T., and da Silva, A. J. (2001). "Dynamics of Dinophysis acuta, D. acuminata, D. tripos and *Gymnodinium catenatum* during an upwelling event off the northwest coast of Portugal," in *Proceedings of the 9th International Conference on Harmful Algal Blooms Hobart*, Australia, 7-11 February 2000. Eds. G. M. Hallegraeff, S. I. Blackbum, C. J. Bolch and R. J. Lewis (Intergovemmental Oceanographic Commission of UNESCO 2001169–172).

Moita, M. T., Oliveira, P. B., Mendes, J. C., and Palma, A. S. (2003). Distribution of chlorophyll a and *Gymnodinium catenatum* associated with coastal upwelling plumes off central Portugal. *Acta Oecol.* 24, S125–S132. doi: 10.1016/S1146-609X(03)00011-0

Moita, T., Oliveira, P. B., Santos, A., Zacarias, N., Borges, C., Palma, C., et al. (2022). "*Protoceratium reticulatum* bloom in NW Iberia mid-shelf waters," in *19th International Conference on Harmful Algae*. Eds. C. J. Band-Schmidt and C. F. Rodríguez-Gómez (La Paz, B.C.S, Mexico: International Society for the Study of Harmful Algal Blooms), pp. 76-81. doi: 10.5281/zenodo.7034945

Moita, M. T., and Vilarinho, M. G. (1999). Checklist of phytoplankton species off Portugal: 70 years, (1929-1998) of studies. *Portugaliae Acta Biol. Sér. B Sist* 18, 5–50.

Montresor, M., and Marino, D. (1996). Modulating effect of cold-dark storage on excystment in Alexandrium pseudogonyaulax (Dinophyceae). *Mar. Biol.* 127 (1), 55–60. doi: 10.1007/BF00993643

Mora, C., and Vieira, G. (2020). "The Climate of Portugal," in *Landscapes and Landforms of Portugal. World Geomorphological Landscapes*. Eds. G. Vieira, J. Zêzere and C. Mora (Cham: Springer). doi: 10.1007/978-3-319-03641-0_2

Mudie, P. J., Marret, F., Mertens, K. N., Shumilovskikh, L., and Leroy, S. A. (2017). Atlas of modern dinoflagellate cyst distributions in the Black Sea Corridor: from Aegean to Aral Seas, including Marmara, Black, Azov and Caspian Seas. *Mar. Micropaleontol.* 134, 1–152. doi: 10.1016/j.marmicro.2017.05.004

Nehring, S. (1996). Recruitment of planktonic dinoflagellates: importance of benthic resting stages and resuspension events. *Internation. Rev. der gesamten Hydrobiol. und Hydrogr.* 81 (4), 513–527. doi: 10.1002/iroh.19960810404

Nolasco, R., Gomes, I., Peteiro, L., Albuquerque, R., Luna, T., Dubert, J., et al. (2018). Independent estimates of marine population connectivity are more concordant when accounting for uncertainties in larval origins. *Sci. Rep.* 8, 2641. doi: 10.1038/s41598-018-19833-w

Nooteboom, P. D., Bijl, P. K., van Sebille, E., Von Der Heydt, A. S., and Dijkstra, H. A. (2019). Transport bias by ocean currents in sedimentary microplankton assemblages: Implications for paleoceanographic reconstructions. *Paleoceanogr. Paleoclimatol.* 34 (7), 1178–1194. doi: 10.1029/2019PA003606

Nunes, P. (2021). Spatial-Temporal distribution of phytoplankton biomass during a coastal upwelling episode obtained from remote sensing and in *situ* data. MSc Thesis (Lisbon: University of Lisbon).

Nunes, P., Nolasco, R., Dubert, J., Brotas, V., and Olivaira, P. B. (2022). "Evidence of upwelling separation from the coast off NW Portugal," in *Instituto Hidrográfico, 2022. Atas das 7as Jornadas de Engenharia Hidrográfica/2as Jornadas Luso-Espanholas de Hidrografia*, Lisboa, 21th–23rd June 2022, pp. 105-108. Available at: https://jornadas.hidrografico.pt/recursos/files/documentos/2022/7JEH-Livro_Atas.pdf.

Oliveira, P. B., Amorim, F. N., Dubert, J., Nolasco, R., and Moita, T. (2019). Phytoplankton distribution and physical processes off NW Iberia during two consecutive upwelling seasons. *Continent. Shelf Res.* 190, 103987. doi: 10.1016/j.csr.2019.103987

Oliveira, P. B., Magalhães, J. M., Pires, A. C., Oliveira, A., and Santos, A. I. (2020). "Mid-shelf internal wave activity off Figueira da Foz in September 2019," in *6as Jornadas de Engenharia Hidrográfica/1as Jornadas Luso-Espanholas de Hidrografia*, Lisboa, 23-25 June 2020, pp. 139-142. Available at: https://jornadas.hidrografico.pt/recursos/files/documentos/Livro_Atas_6JEH_2020.pdf.

Oliveira, P. B., Moita, T., Silva, A., Monteiro, I. T., and Palma, A. S. (2009b). Summer diatom and dinoflagellate blooms in Lisbon Bay from 2002 to 2005: Pre-conditions inferred from wind and satellite data. *Prog. Oceanogr.* 83 (1–4), 270–277. doi: 10.1016/j.pocean.2009.07.030

Oliveira, P. B., Nolasco, R., Dubert, J., Moita, T., and Peliz, Á. (2009a). Surface temperature, chlorophyll and advection patterns during a summer upwelling event off central Portugal. *Continent. Shelf Res.* 29 (5–6), 759–774. doi: 10.1016/j.csr.2008.08.004

Oliveira, A., Santos, A. I., Oliveira, P. B., Zacarias, N., and Amorim, A. (2020). "Dynamics of Nepheloid layers associated with internal wave activity off Figueira da Foz," in *6as Jornadas de Engenharia Hidrográfica/1as Jornadas Luso-Espanholas de Hidrografia*, Lisboa, 23-25 June 2020 pp. 273-275. Available at: https://jornadas.hidrografico.pt/recursos/files/documentos/Livro_Atas_6JEH_2020.pdf.

Oliveira, A., Santos, A. I., Rodrigues, A., and Vitorino, J. (2007). Sedimentary particle distribution and dynamics on the Nazaré canyon system and adjacent shelf (Portugal). *Mar. Geol.* 246 (2), 105–122. doi: 10.1016/j.margeo.2007.04.017

Oliveira, A., Santos, A. I., Santos, R., and Zacarias, N. (2023). Nepheloid layer dynamics overview of the Portuguese continental shelf. *Continent. Shelf Res.* 261, 105027. doi: 10.1016/j.csr.2023.105027

Oliveira, A., Vitorino, J., Rodrigues, A., Jouanneau, J. M., Dias, J. A., and Weber, O. (2002). Nepheloid layer dynamics in the northern Portuguese shelf. *Prog. Oceanogr.* 52 (2–4), 195–213. doi: 10.1016/S0079-6611(02)00006-X

Otero, P., Ruiz-Villarreal, M., and Peliz, A. (2008). Variability of river plumes off Northwest Iberia in response to wind events. *J. Mar. Syst.* 72 (1–4), 238–255. doi: 10.1016/j.jmarsys.2007.05.016

Peliz, Á., Dubert, J., Santos, A. M. P., Oliveira, P. B., and Le Cann, B. (2005). Winter upper ocean circulation in the Western Iberian Basin—Fronts, Eddies and Poleward Flows: an overview. *Deep sea Res. Part I: Oceanogr. Res. papers* 52 (4), 621–646. doi: 10.1016/j.dsr.2004.11.005

Peliz, A., Rosa, T., Santos, A. M. P., and Pissara, J. L. (2002). Fronts, jets, and counterflows in the Western Iberian upwelling system. *J. Mar. Syst.* 35, 61–77. doi: 10.1016/s0924-7963(02)00076-3

Peña-Manjarrez, J. L., Gaxiola-Castro, G., and Helenes-Escamilla, J. (2009). Environmental factors influencing the variability of Lingulodinium polyedrum and Scrippsiella trochoidea (Dinophyceae) cyst production. *Cienc. Marinas* 35 (1), 1–14. doi: 10.7773/cm.v35i1.1406

Pfiester, L. A., and Anderson, D. M. (1987). "Dinoflagellate reproduction," in *The Biology of Dinoflagellates*. Ed. F. J. R. Taylor (Oxford: Blackwell Scientific), 611–648.

Pilskaln, C. H., Anderson, D. M., McGillicuddy, D. J., Keafer, B. A., Hayashi, K., and Norton, K. (2014a). Spatial and temporal variability of *Alexandrium* cyst fluxes in the Gulf of Maine: relationship to seasonal particle export and resuspension. *Deep Sea Res. Part II: Topical Stud. Oceanogr.* 103, 40–54. doi: 10.1016/j.dsr2.2012.11.001

Pilskaln, C. H., Hayashi, K., Keafer, B. A., Anderson, D. M., and McGillicuddy, D. J.Jr. (2014b). Benthic nepheloid layers in the Gulf of Maine and *Alexandrium* cyst inventories. *Deep Sea Res. Part II Topical Stud. Oceanogr.* 103, 55–65. doi: 10.1016/j.dsr2.2013.05.021

Pitcher, G. C., Figueiras, F. G., Hickey, B. M., and Moita, M. T. (2010). The physical oceanography of upwelling systems and the development of harmful algal blooms. *Prog. Oceanogr.* 85, 5–32. doi: 10.1016/j.pocean.2010.02.002

Pospelova, V., and Head, M. J. (2002). *Islandinium brevispinosum* sp. nov. (Dinoflagellata), a new organic-walled dinoflagellate cyst from modern estuarine sediments of New England (USA). *J. Phycol.* 38 (3), 593–601. doi: 10.1046/j.1529-8817.2002.01206.x

Price, A. M., and Pospelova, V. (2011). High-resolution sediment trap study of organic-walled dinoflagellate cyst production and biogenic silica flux in Saanich Inlet (BC, Canada). *Mar. Micropaleontol.* 80 (1–2), 18–43. doi: 10.1016/j.marmicro.2011.03.003

Quaresma, L. S., Vitorino, J., Oliveira, A., and da Silva, J. (2007). Evidence of sediment resuspension by nonlinear internal waves on the western Portuguese mid-shelf. *Mar. geol.* 246 (2–4), 123–143. doi: 10.1016/j.margeo.2007.04.019

Radi, T., Bonnet, S., Cormier, M.-A., de Vernal, A., Durantou, L., Faubert, É., et al. (2013). Operational taxonomy and (paleo-)autecology of round, brown, spiny dinoflagellate cysts from the Quaternary of high northern latitudes. *Mar. Micropaleontol.* 98, 41–57. doi: 10.1016/j.marmicro.2012.11.001

R Development Core Team. (2013). *R: A Language and Environment for Statistical Computing* (Vienna, Austria: R Foundation for Statistical Computing). Available at: http://www.Rproject.org.

Relvas, P., Barton, E. D., Dubert, J., Oliveira, P. B., Peliz, A., Da Silva, J. C. B., et al. (2007). Physical oceanography of the western Iberia ecosystem: latest views and challenges. *Prog. Oceanogr.* 74, 149–173. doi: 10.1016/j.pocean.2007.04.021

Rengefors, K., Gustafsson, S., and Ståhl-Delbanco, A. (2004). Factors regulating the recruitment of cyanobacterial and eukaryotic phytoplankton from littoral and profundal sediments. *Aquat. Microbial. Ecol.* 36, 213–226. doi: 10.3354/ame036213

Ribeiro, S., Amorim, A., Andersen, T. J., Abrantes, F., and Ellegaard, M. (2012). Reconstructing the history of an invasion: the toxic phytoplankton species *Gymnodinium catenatum* in the Northeast Atlantic. *Biol. Invasions* 14, 969–985. doi: 10.1007/s10530-011-0132-6

Rossi, V., Garçon, V., Tassel, J., Romagnan, J. B., Stemmann, L., Jourdin, F., et al. (2013). Cross-shelf variability in the Iberian Peninsula Upwelling System: Impact of a mesoscale filament. *Continent. Shelf Res.* 59, 97–114. doi: 10.1016/j.csr.2013.04.008

Salgado, P., Figueroa, R. I., Ramilo, I., and Bravo, I. (2017). The life history of the toxic marine dinoflagellate *Protoceratium reticulatum* (Gonyaulacales) in culture. *Harmful Algae* 68, 67–81. doi: 10.1016/j.hal.2017.07.008

Santos, A. I., Magalhães, J., Oliveir, A., Oliveira, P. B., Zacarias, N. R., and Amorim, A. (2022). "ADCP backscattering patterns in a mid-shelf water column (Figueira da Foz – W Portugal): Interaction between physical/biological forcing and particle dynamics," in *Instituto Hidrográfico, 2022. Atas das 7as Jornadas de Engenharia Hidrográfica/2as Jornadas Luso-Espanholas de Hidrografia*, Lisboa, 21th-23th June 2022, pp. 141-144. Available at: https://jornadas.hidrografico.pt/recursos/files/documentos/2022/7JEH-Livro_Atas.pdf.

Santos, M., Moita, M. T., Oliveira, P. B., and Amorim, A. (2021). Phytoplankton communities in two wide-open bays in the Iberian upwelling system. *J. Sea Res.* 167, 101982. doi: 10.1016/j.seares.2020.101982

Smayda, T. J. (1971). Normal and accelerated sinking of phytoplankton in the sea. *Mar. Geol.* 11 (2), 105–122. doi: 10.1016/0025-3227(71)90070-3

Smayda, T. J., and Reynolds, C. S. (2001). Community assembly in marine phytoplankton: application of recent models to harmful dinoflagellate blooms. *J. Plankton Res.* 23 (5), 447–461.

Smayda, T. J. (2002). Turbulence, watermass stratification and harmful algal blooms: an alternative view and frontal zones as "pelagic seed banks". *Harmful Algae* 1 (1), 95–112. doi: 10.1016/S1568-9883(02)00010-0

Smayda, T. J., and Reynolds, C. S. (2003). Strategies of marine dinoflagellate survival and some rules of assembly. *J. Sea Res.* 49 (2), 95–106. doi: 10.1016/S1385-1101(02)00219-8

Smayda, T. J., and Trainer, V. L. (2010). Dinoflagellate blooms in upwelling systems: seeding, variability, and contrasts with diatom bloom behaviour. *Prog. Oceanogr.* 85, 92–107. doi: 10.1016/j.pocean.2010.02.006

Susek, E., Zonneveld, K. A., Fischer, G., Versteegh, G. J., and Willems, H. (2005). Organic-walled dinoflagellate cyst production in relation to upwelling intensity and lithogenic influx in the Cape Blanc region (off north-west Africa). *Phycological Res.* 53 (2), 97–112.

Suzuki, R., Terada, Y., and Shimodaira, H. (2022) *Hierarchical Clustering with P-Values via Multiscale Bootstrap Resampling, V. 2.2-0. Cran repository*. Available at: http://stat.sys.i.kyoto-u.ac.jp/prog/pvclust/.

Teles-MaChado, A., Peliz, A., CcWilliams, J. C., Cardoso, R. M., Soares, P. M. M., and Miranda, P. M. A. (2015). On the year-to-year changes of the Iberian Poleward Current. *J. Geophys. Res.: Oceans* 120, 4980–4999. doi: 10.1002/2015JC010758

Thomsen, L., vanWeering, T., and Gust, G. (2002). Processes in the benthic boundary layer at the Iberian continental margin and their implication for carbon mineralization. *Prog. Oceanogr.* 52 (2–4), 315–329. doi: 10.1016/S0079-6611(02)00013-7

Tian, Z., Liu, Y., Zhang, X., Zhang, Y., and Zhang, M. (2022). Formation mechanisms and characteristics of the marine nepheloid layer: A review. *Water* 14 (5), 678. doi: 10.3390/w14050678

Tilstone, G. H., Figueiras, F. G., and Fraga, F. (1994). Upwelling-downwelling sequences in the generation of red tides in a coastal upwelling system. *Mar. Ecol. Prog. Series. Oldendorf* 112 (3), 241–253. doi: 10.3354/meps112241

Tilstone, G. H., Miguez, B. M., Figueiras, F. G., and Fermín, E. G. (2000). Diatom dynamics in a coastal ecosystem affected by upwelling: coupling between species succession, circulation and biogeochemical processes. *Mar. Ecol. Prog. Ser.* 205, 23–41. doi: 10.3354/meps205023

Trainer, V. L., Pitcher, G. C., Reguera, B., and Smayda, T. J. (2010). The distribution and impacts of harmful algal bloom species in eastern boundary upwelling systems. *Prog. Oceanogr.* 85 (1–2), 33–52. doi: 10.1016/j.pocean.2010.02.003

Turner, J. T. (2002). Zooplankton fecal pellets, marine snow and sinking phytoplankton blooms. *Aquat. Microbiol. Ecol.* 27, 57–102. doi: 10.3354/ame027057

van Nieuwenhove, N., Head, M. J., Limoges, A., Pospelova, V., Mertens, K. N., Matthiessen, J., et al. (2020). An overview and a brief description of common marine organic-walled dinoflagellate cyst taxa occurring in surface sediments of the Northern Hemisphere. *Mar. Micropaleontol.* 159, 101814. doi: 10.1016/j.marmicro.2019.101814

Venrick, E. L. (1978). "Sampling strategies," in *Phytoplankton Manual. Monographs on Oceanic Methodology*, vol. 6 . Ed. A. Sournia (Paris: UNESCO), 7–16.

Villacieros-Robineau, N., Zúñiga, D., Barreiro-González, B., Alonso-Pérez, F., de la Granda, F., Froján, M., et al. (2019). Bottom boundary layer and particle dynamics in an upwelling affected continental margin (NW Iberia). *J. Geophys. Res.: Oceans* 124, 9531. doi: 10.1029/2019JC015619

Vitorino, J., Oliveira, A., Jouanneau, J. M., and Drago, T. (2002). Winter dynamics on the northern Portuguese shelf: Part 2: bottom boundary layers and sediment. *Prog. Oceanogr.* 52 (2-4), 155–170. doi: 10.1016/S0079-6611(02)00004-6

Waite, A. M., Safi, K. A., Hall, J. A., and Nodder, S. D. (2000). Mass sedimentation of picoplankton embedded in organic aggregates. *Limnol. Oceanogr.* 45 (1), 87–97. doi: 10.4319/lo.2000.45.1.0087

Zonneveld, K. A. F., and Brummer, G.-J. A. (2000). (Palaeo-)ecological significance, transport and preservation of organic-walled dinoflagellate cysts in the Somali Basin, NW Arabian Sea. *Deep-Sea Res. II* 47, 2229–2256. doi: 10.1016/S0967-0645(00)00023-0

Zonneveld, K. A. F., Ebersbach, F., Maeke, M., and Versteegh, G. J. M. (2018). Transport of organic-walled dinoflagellate cysts in nepheloid layers off Cape Blanc (N-W Africa). *Deep-Sea Res. Part I* 139, 55–67. doi: 10.1016/j.dsr.2018.06.003

Zonneveld, K. A., Grotheer, H., and Versteegh, G. J. (2022). Dinoflagellate cysts production, excystment and transport in the upwelling off Cape Blanc (NW Africa). *Front. Mar. Sci.* 1317. doi: 10.3389/fmars.2022.915755

Zonneveld, K. A. F., Meilland, J., Donner, B., and Versteegh, G. J. M. (2021). Export flux succession of dinoflagellate cysts and planktonic foraminifera in an active upwelling cell off Cape Blanc (NW Africa). *Eur. J. Phycol.* 57 (1), 29-47. doi: 10.1080/09670262.2021.1885066

Zonneveld, K. A. F., and Pospelova, V. (2015). A determination key for modern dinoflagellate cysts. *Palynology* 39 (3), 387–409. doi: 10.1080/01916122.2014.990115

Zonneveld, K. A., Versteegh, G., and Kodrans-Nsiah, M. (2008). Preservation and organic chemistry of late Cenozoic organic-walled dinoflagellate cysts: a review. *Mar. Micropaleontol.* 68 (1–2), 179–197. doi: 10.1016/j.marmicro.2008.01.015

Zonneveld, K. A., Susek, E., and Fischer, G. (2010). Seasonal variability of the organic-walled dinoflagellate cyst production in the coastal upwelling region off Cape Blanc (Mauritania): a five-year survey. *J. Phycology* 46 (1), 202–215.